

Smooth backfitting of proportional hazards with multiplicative components

Munir Hiabu ^{*1}, Enno Mammen², M. Dolores Martínez-Miranda³ and Jens
P. Nielsen⁴

¹School of Mathematics and Statistics, University of Sydney, Camperdown
NSW 2006, Australia

²Institute for Applied Mathematics, Heidelberg University, Im Neuenheimer
Feld 205, 69120 Heidelberg, Germany

³Department of Statistics and Operations Research, University of Granada,
Campus Fuentenueva s/n. 18071 Granada, Spain

⁴Cass Business School, City, University of London, 106 Bunhill Row,
London, EC1Y 8TZ, United Kingdom

February 7, 2020

*munir.hiabu@sydney.edu.au (Corresponding author)

Acknowledgement: We are grateful to the authors of Lin et al. (2016), who provided us with code for the calculation of their estimator.

Abstract

Smooth backfitting has proven to have a number of theoretical and practical advantages in structured regression. By projecting the data down onto the structured space of interest smooth backfitting provides a direct link between data and estimator. This paper introduces the ideas of smooth backfitting to survival analysis in a proportional hazard model, where we assume an underlying conditional hazard with multiplicative components. We develop asymptotic theory for the estimator. In a comprehensive simulation study we show that our smooth backfitting estimator successfully circumvents the curse of dimensionality and outperforms existing estimators. This is especially the case in difficult situations like high number of covariates and/or high correlation between the covariates, where other estimators tend to break down. We use the smooth backfitter in a practical application where we extend recent advances of in-sample forecasting methodology by allowing more information to be incorporated, while still obeying the structured requirements of in-sample forecasting.

1 Introduction

Nonparametric models suffer from the curse of dimensionality in high dimensional data spaces. Random forests (Breiman, 2001) circumvent the dimensionality problem by assuming that not all variables are relevant and that the function of interest can be approximated well by piecewise constant functions; see Wright and Ziegler (2017) for a recent survival implementation. An alternative is to introduce some structure that stabilizes the system. Introducing structure has the additional advantage that it allows to visualize, interpret, extrapolate and forecast the properties of the underlying data. In this paper, we concentrate on structured models. The smooth backfitting algorithm of Mammen et al. (1999) considers the simplest nonparametric structure in the regression context - the additive structure. It has many theoretical and practical advantages to earlier approaches of regression backfitting.

The popular regression backfitting approach of Hastie and Tibshirani (1990a) are numerical iterating-procedures estimating one component given the estimates of the rest. In contrast, smooth backfitting is a direct projection of the data down onto the structured space of interest. This direct relationship between data and estimates gives a more solid grip on what is being estimated and the theoretical properties underlying it, see also Nielsen and Sperlich (2005) and Huang and Yu (2019). The purpose of this paper is to introduce smooth backfitting to the field of survival analysis and nonparametric smooth hazard estimation. While the additive structure is the most natural and most widely used in regression, the multiplicative structure seems more natural in hazard estimation. The omnipresent Cox regression model is a proportional hazard model (also known as Cox proportional hazard model) and many extensions and alternatives to the Cox regression model have been formulated in a multiplicative framework. We will therefore consider the multiplicative structure in this paper. It can be used in applications to test Cox regression or other proportional hazard models either visually or quantitatively. But this is beyond the scope of this paper. Multiplicative smooth backfitting is theoretically more challenging than additive smooth backfitting. The smooth backfitting multiplicative regression structure was analysed by Yu et al. (2008) as a special case of generalized additive models. Yu et al. (2008) showed that the multiplicative structure - in contrast to the simpler additive case - provides asymptotic theory with a number of non-trivial interactions between exposure available in different directions. Naturally, the asymptotics provided here for smooth backfitting of multiplicative hazards contains similar interactive components in the asymptotic theory. The survival projection introduced in this paper is different and less intuitive than the nonparametric regression considered in Mammen et al. (1999, 2001). As in density estimation, see Jones (1993), hazard estimation requires a projection of a dirac-delta-sequence related to the jumps of the counting process, see also Nielsen (1998) and Nielsen and Tanggaard (2001). We provide a simple algorithm first projecting the data down onto an unstructured estimator, and then further projecting

the unstructured estimator down onto the multiplicative space of interest. Our numerical algorithms are greatly simplified by a new principle of weighting the projection according to the final estimates.

We consider a multiplicatively structured proportional hazard model:

$$\alpha(t, z) = \alpha_0(t)\alpha_1(z_1) \cdots \alpha_d(z_d), \tag{1.1}$$

where α_k , $k = 0, \dots, d$, are some smooth and positive one-dimensional functions and $z = (z_1, \dots, z_d) \in \mathbb{R}^d$ are possibly time t -dependent covariates. We do not impose any further structural assumption on α_k . This is in contrast to the semiparametric Cox proportional hazard model where all components, with exception of the baseline hazard α_0 , are assumed to take a log-linear shape. We do expect that smooth backfitting of proportional hazard models can be generalized to much the same way as the Cox proportional hazard model is generalized. As one recent example that could be interesting to treat as a smooth backfitting problem, see Hsu et al. (2018).

Estimators for model (1.1) can be categorized in four groups: (i) Therneau et al. (1990) and Grambsch et al. (1995) start with the Cox model and investigate smoothed residual plots; (ii) Hastie and Tibshirani (1990a,b), OSullivan (1988, 1993), Sleeper and Harrington (1990) and Huang (1999) consider splines via penalized partial likelihood; (iii) Linton et al. (2003), Honda (2005) build on marginal integration (Linton and Nielsen, 1995) and (iv) Lin et al. (2016) use kernel smoothers starting from a global partial likelihood criterion.

Lin et al. (2016) prove asymptotic efficiency of their estimator and they show by a detailed simulation study that their estimator outperforms the proposals in Huang (1999), Linton et al. (2003), Honda (2005). For this reason in this paper we take their estimator as benchmark. It has been argued that in additive regression models smooth backfitting is less affected by sparseness of high-dimensional data and by strong correlated covariables, see

Nielsen and Sperlich (2005). In this paper we will show that this also holds for our smooth backfitter in a multiplicatively structured proportional hazard model. For this purpose we study the smooth backfitter in settings which include challenging high dimensional data and highly correlated covariates. The smooth backfitting approach turns out to show a very good performance compared to all other estimators and to be very robust to both, high dimensional and correlated data. In particular in high-dimensional settings it strongly outperforms the approach of Lin et al. (2016) that already for low dimensions runs into instabilities and numerical problems. In this paper, we do not treat the problem of variable selection. It would in particular be interesting to investigate Lasso approaches or nonparametric tests on the significance of one component. For the development of tests our theory may be used as a first step.

The paper is structured as follows. Section 2 contains the mathematics of the underlying survival model. In Section 3 the smooth backfitting estimator is defined as a projection of unstructured hazard estimators. This is done for unstructured hazard estimators that can be written as a ratio of smooth occurrence and smooth exposure. An example is given by the local constant Nadaraya-Watson estimator. In Section 4 asymptotic properties are outlined for the smooth backfitting estimator. Details are explained in the Supplementary Material of this paper. Section 5 contains our finite sample study illustrating the strong performance of smooth backfitting. In Section 6 we consider a sophisticated version of in-sample forecasting generalising earlier approaches via our proportional hazard model, see Mammen et al. (2015), Hiabu et al. (2016) Lee et al. (2015, 2017, 2018). A smooth extension of the popular actuarial chain ladder model that is used in virtually all non-life insurance companies in the world while estimating outstanding liabilities. In-sample forecasting is possible because of the imposed multiplicative structure.

2 Aalen's multiplicative intensity model

We consider a counting process formulation satisfying Aalen's multiplicative intensity model. It allows for very general observations schemes. It covers filtered observations arising from left truncation and right censoring and also more complicated patterns of occurrence and exposure. In the next section we describe how to embed left truncation and right censoring into this framework. In contrast to Linton et al. (2003) we will hereby allow the filtering to be correlated to the survival time and be represented in the covariate process. We briefly summarize the general model we are assuming.

We observe n *iid* copies of the stochastic processes $(N(t), Y(t), Z(t))$, $t \in [0, R_0]$, $R_0 > 0$. Here, N denotes a right-continuous counting process which is zero at time zero and has jumps of size one. The process Y is left-continuous and takes values in $\{0, 1\}$ where the value 1 indicates that the individual is under risk. Finally, Z is a d -dimensional left-continuous covariate process with values in a hyperrectangle $\prod_{j=1}^d [0, R_j] \subset \mathbb{R}^d$. The multivariate process $((N_1, Y_1, Z_1), \dots, (N_n, Y_n, Z_n))$, $i = 1, \dots, n$, is adapted to the filtration \mathcal{F}_t which satisfies the usual conditions (the usual conditions), see Andersen et al. (1993) (pp. 60). Now we assume that N_i satisfies Aalen's multiplicative intensity model, that is

$$\lambda_i(t) = \lim_{h \downarrow 0} h^{-1} E[N_i((t+h)-) - N_i(t-) | \mathcal{F}_{t-}] = \alpha(t, Z_i(t)) Y_i(t). \quad (2.1)$$

The deterministic function $\alpha(t, z)$ is called hazard function and it is the failure rate of an individual at time t given the covariate $Z(t) = z$.

2.1 Left truncation and right censoring time as covariates

The most prominent example for Aalen's multiplicative intensity model is filtered observation due to left truncation and right censoring. We now show how to embed model (1.1)

with covariate, Z , possibly carrying truncation and censoring information into Aalen's multiplicative intensity model. Every covariate coordinate can carry individual truncation information as long as it corresponds to left truncation. That is, we observe (T, Z) if and only if $(T, Z(T)) \in \mathcal{I}$, where the set \mathcal{I} is compact and it holds that if $(t_1, Z(t_1)) \in \mathcal{I}$ and $t_2 \geq t_1$, then $(t_2, Z(t_2)) \in \mathcal{I}$, *a.s.* The set \mathcal{I} is allowed to be random but is independent of T given the covariate process Z . Furthermore, T can be subject to right censoring with censoring time C . We assume that also T and C are conditional independent given the covariate process Z . This includes the case where the censoring time equals one covariate coordinate. In conclusion, we observe n *iid* copies of $(\tilde{T}, Z^*, \mathcal{I}, \delta)$, where $\delta = \mathbb{1}(T^* < C)$, $\tilde{T} = \min(T^*, C)$, and (T^*, Z^*) is the truncated version of (T, Z) , i.e., (T^*, Z^*) arises from (T, Z) by conditioning on the event $(T, Z(T)) \in \mathcal{I}$.

Then, for each subject, $i = 1, \dots, n$, we can define a counting process N_i as $N_i(t) = \mathbb{1} \left\{ \tilde{T}_i \leq t, \delta_i = 1 \right\}$, with respect to the filtration $\mathcal{F}_{i,t} = \sigma \left(\left\{ \tilde{T}_i \leq s, Z_i^*(s), \mathcal{I}_i, \delta_i : s \leq t \right\} \cup \mathcal{N} \right)$, where \mathcal{N} is a class of null-sets that completes the filtration. After straightforward computations one can conclude that under the setting above, Aalen's multiplicative intensity model (2.1) is satisfied with

$$\alpha_z(t) = \alpha(t, z) = \lim_{h \downarrow 0} h^{-1} \Pr \{ T_i \in [t, t+h] \mid T_i \geq t, Z_i(t) = z \},$$

$$Y_i(t) = \mathbb{1} \{ (t, Z_i^*(t)) \in \mathcal{I}_i, t \leq \tilde{T}_i \}.$$

3 Estimation

We tackle the problem in two steps. First the data are projected down onto an unstructured space resulting in an unstructured estimator of the $d+1$ -dimensional hazard function $\alpha(t, z)$; see (1.1). In the second step, the unstructured estimator is projected further down onto the multiplicative space of interest resulting in $d+1$ one-dimensional smooth backfitting

estimators of the multiplicative components, $(\alpha_0(t), \alpha_1(z_1), \dots, \alpha_d(z_d))$. For the first step we assume to have an unstructured estimator with simple ratio of smoothed occurrence and smoothed exposure. Our theory will encompass all estimators with this simple ratio structure. We discuss in Section A and in the accompanied Supplementary Material that our estimation procedure works under quite general assumptions. In particular we do not need the unstructured estimator of the first step to be consistent. The final structured estimator circumvents the curse of dimensionality even if consistency is not assured in the first step. This is reassuring noting that the unstructured estimator will most probably have exponentially deteriorating performance with growing dimension d .

We introduce the notation $X_i(t) = (t, Z_i(t))$. We also set $x = (t, z)$, with coordinates $x_0 = t$, $x_1 = z_1, \dots, x_d = z_d$, and write the hazard as $\alpha(t, z) = \alpha(x)$.

3.1 First step: The unstructured estimator

To estimate the components of the structured hazard in (3.2) below, we will need an unstructured pilot estimator of the hazard α first. We propose the local constant kernel estimator, $\tilde{\alpha}^{LC}$. Its value in x is defined as

$$\begin{aligned} \tilde{\alpha}^{LC}(x) = \lim_{\varepsilon \rightarrow 0} \arg \min_{\theta_0 \in \mathbb{R}} \sum_{i=1}^n \int \left\{ \frac{1}{\varepsilon} \int_s^{s+\varepsilon} dN_i(u) - \theta_0 \right\}^2 \\ \times \kappa_n(X_i(s)) K_b(x - X_i(s)) Y_i(s) ds. \end{aligned} \quad (3.1)$$

In the following, we restrict ourselves to a multiplicative kernel, i.e., for $(u_0, \dots, u_d) \in \mathbb{R}^{d+1}$, $K(u_0, \dots, u_d) = \prod_{j=0}^d k(u_j)$, and a one-dimensional bandwidth b with boundary correction $\kappa_n(x) = \prod_{j=0}^d \left(\int K_b(x_j - u_j) du_j \right)^{-1}$ and $K_b(u) = \prod_{j=0}^d b^{-1} k(b^{-1} u_j)$, where for simplicity of notation the bandwidth $b > 0$ does not depend on j . More general choices would have been possible with the cost of extra notation.

We get $\tilde{\alpha}^{LC}(x) = \widehat{O}^{LC}(x)/\widehat{E}^{LC}(x)$, with smoothed occurrence and smoothed exposure given by

$$\begin{aligned}\widehat{O}^{LC}(x) &= \sum_{i=1}^n \int \kappa_n(X_i(s)) K_b(x - X_i(s)) dN_i(s), \\ \widehat{E}^{LC}(x) &= \sum_{i=1}^n \int \kappa_n(X_i(s)) K_b(x - X_i(s)) Y_i(s) ds.\end{aligned}$$

Under standard smoothing conditions, if b is chosen of order $n^{-1/(4+d+1)}$, then the bias of $\tilde{\alpha}^{LC}(x)$ is of order $n^{-2/(4+d+1)}$ and the variance is of order $n^{-4/(4+d+1)}$, which is the optimal rate of convergence in the corresponding regression problem, see Stone (1982). For an asymptotic theory of these estimators see Linton et al. (2003).

3.2 Second step: The structured smooth backfitting estimator

In this section we will project the unstructured estimator of the previous section down onto the multiplicative space of interest. Other choices that have a simple ratio structure of occurrence and exposure are possible. Due to filtering, observations are assumed to be only available on a subset of the full support, $\mathcal{X} \subseteq \mathcal{R} = \prod_{j=0}^d [0, R_j]$. Our estimators are restricted to this set and detailed assumptions on \mathcal{X} and the data generating functions are given in the Supplementary Material. Our calculations simplify via a new principle we call solution-weighted minimization. We assume that we have the solution and use it strategically in the least squares weighting. While the definition is not explicit, it is made feasible by defining it as an iterative procedure. In the sequel we will assume a multiplicative structure of the hazard α , i.e.,

$$\alpha(x) = \alpha^* \prod_{j=0}^d \alpha_j(x_j), \quad (3.2)$$

where α_j , $j = 0, \dots, d$, are some functions and α^* is a constant. For identifiability of the components, we make the following further assumption:

$$\int \alpha_j(x_j)w_j(x_j) dx_j = 1, \quad j = 0, \dots, d,$$

where the w_j 's are some weight functions.

We also need the following notation:

$$F_t(z) = Pr(Z_1(t) \leq z | Y_1(t) = 1), \quad y(t) = E[Y_1(t)].$$

By denoting $f_t(z)$ the density corresponding to $F_t(z)$ with respect to the Lebesgue measure, we also define $E(x) = f_t(z)y(t)$ and $O(x) = E(x)\alpha(x)$.

We define the estimators $\hat{\alpha}^*$ and $\hat{\alpha} = (\hat{\alpha}_0, \dots, \hat{\alpha}_d)$ of the hazard components in (3.2) as solution of the following system of equations:

$$\hat{\alpha}_k(x_k) = \frac{\int_{\mathcal{X}_{x_k}} \hat{O}(x) dx_{-k}}{\int_{\mathcal{X}_{x_k}} \hat{\alpha}^* \prod_{j \neq k} \hat{\alpha}_j(x_j) \hat{E}(x) dx_{-k}}, \quad k = 0, \dots, d, \quad (3.3)$$

$$\int \hat{\alpha}_k(x_k)w_k(x_k) dx_k = 1, \quad k = 0, \dots, d. \quad (3.4)$$

Here \mathcal{X}_{x_k} denotes the set $\{(x_0, \dots, x_{k-1}, x_{k+1}, \dots, x_d) | (x_0, \dots, x_d) \in \mathcal{X}\}$, and $x_{-k} = (x_0, \dots, x_{k-1}, x_{k+1}, \dots, x_d)$. Furthermore, \hat{E} and \hat{O} are some full-dimensional estimators of E and O – not necessarily the one provided in the previous section. We will discuss in the Supplementary Material that the system above has a solution with probability tending to one. In the next section and in the Supplementary Material we will show asymptotic properties of the estimator. We will see that we do not require that the full-dimensional estimators \hat{E} and \hat{O} are consistent. We will only need asymptotic consistency of marginal averages of the estimators. This already highlights that our estimator efficiently circumvents

the curse of dimensionality.

In practice, system (3.3) can be solved by the following iterative procedure:

$$\widehat{\alpha}_k^{(r+1)}(x_k) = \frac{\int_{\mathcal{X}_{x_k}} \widehat{O}(x) dx_{-k}}{\int_{\mathcal{X}_{x_k}} \prod_{j=0}^{k-1} \widehat{\alpha}_j^{(r+1)}(x_j) \prod_{j=k+1}^{d+1} \widehat{\alpha}_j^{(r)}(x_j) \widehat{E}(x) dx_{-k}}, \quad k = 0, \dots, d \quad (3.5)$$

After a finite number of cycles or after a termination criterion applies, the last values of $\widehat{\alpha}_k^{(r+1)}(x_k)$, $k = 0, \dots, d$, are multiplied by a factor such that the constraint (3.4) is fulfilled. This can always be achieved by multiplication with constants. This gives the backfitting approximations of $\widehat{\alpha}_k(x_k)$ for $k = 0, \dots, d$.

3.3 Interpretation as direct projection

The strength of our smooth backfitting estimator is that it can be motivated directly from a least squares criterium on the data without ad-hoc adjustment. The estimator $\widehat{\alpha}$ can be motivated as solution of

$$\lim_{\varepsilon \rightarrow 0} \arg \min_{\theta} \sum_{i=1}^n \int \int \left\{ \frac{1}{\varepsilon} \int_s^{s+\varepsilon} dN_i(u) - \theta(x) \right\}^2 \times K_b(x - X_i(s)) Y_i(s) ds d\nu(x), \quad (3.6)$$

where θ runs over some space of smooth multiplicative functions of the form $\theta = \prod_{j=0}^d \theta_j(x_j)$.

To see this, consider the estimator $\bar{\alpha} = (\bar{\alpha}^*, \bar{\alpha}_0, \dots, \bar{\alpha}_d)$ that minimizes

$$\arg \min_{\bar{\alpha}} \int_{\mathcal{X}} \left\{ \widetilde{\alpha}^{LC}(x) - \bar{\alpha}^* \prod_{j=0}^d \bar{\alpha}_j(x_j) \right\}^2 w(x) dx. \quad (3.7)$$

For $\nu(x) = w(x)/\widehat{E}^{LC}(x) dx$ the solution of (3.7) is exactly (3.6). With that choice, we get

$$\bar{\alpha}^* = \frac{\int_{\mathcal{X}} \widetilde{\alpha}(x) \prod_{j=0}^d \bar{\alpha}_j(x_j) w(x) dx}{\int_{\mathcal{X}} \left\{ \prod_{j=0}^d \bar{\alpha}_j(x_j) \right\}^2 w(x) dx},$$

and $(\bar{\alpha}_0, \dots, \bar{\alpha}_d)$ can be described via the backfitting equation

$$\bar{\alpha}_k(x_k) = \frac{\int_{\mathcal{X}_{x_k}} \tilde{\alpha}(x) \prod_{j \neq k} \bar{\alpha}_j(x_j) w(x) dx_{-k}}{\int_{\mathcal{X}_{x_k}} \bar{\alpha}^* \left\{ \prod_{j \neq k} \bar{\alpha}_j(x_j) \right\}^2 w(x) dx_{-k}}, \quad k = 0, \dots, d. \quad (3.8)$$

The asymptotic variance of kernel estimators of α is proportional to $\alpha(x)/E(x)$, see e.g. Linton and Nielsen (1995). This motivates the choice $w(x) = E(x)/\alpha(x)$. However, this choice is not possible because $E(x)$ and $\alpha(x)$ are unknown. One could use $w(x) = \check{E}(x)/\check{\alpha}(x)$ where $\check{E}(x)$ and $\check{\alpha}(x)$ are some pilot estimators of E and α . We follow another idea and we propose to weight the minimization (3.7) with its solution. We choose

$$w(x) = \frac{\hat{E}(x)}{\prod_i \hat{\alpha}_i(x)}, \quad (3.9)$$

and heuristically, by putting $\bar{\alpha}_j = \hat{\alpha}_j$ and by plugging (3.9) into (3.8), we get (3.3).

4 Asymptotic properties of the smooth backfitter of multiplicative hazards

In the Supplementary Material we show that $\hat{\alpha}_j$ converges to the true α_j with optimal one dimensional nonparametric rate $n^{-2/5}$, given that the bandwidth b is chosen of order $n^{-1/5}$. This means in particular that the asymptotic rate does not depend on the dimension d . Under regularity assumptions, in Theorem 3 in the Supplementary Material we show that

$$n^{2/5} \{(\hat{\alpha}_j - \alpha_j)(x_j) - \alpha_j(x_j) B_j(x_j)\} \rightarrow N(0, \alpha_j^2(x_j) \sigma_j^2(x_j)),$$

where $B_j(x_j)$ can be formally defined as the j -th component of a projection of the bias of the unconstrained estimator onto the multiplicative space and $\sigma_j^2(x_j)$ is the variance of a

weighted average of the unconstrained estimator where the other components are integrated out.

In the simulation study of the next section we show that estimation seems to work well even when d is of similar order as n . This is, we believe, a major strength of our smooth backfitting estimator.

A few notes on the proof. The estimator $\hat{\alpha}_j$ is defined as solution of a nonlinear operator equation. Asymptotic properties are derived by approximating the estimators of this equation by a linear equation that can be interpreted as one equation that arises in nonparametric additive regression models (Mammen et al., 1999), and then one shows that the solution of the linear equation approximates the estimation error in the multiplicative model. The linear equation and its solution is well understood from the theory of additive models. This is our essential step to arrive at an asymptotic understanding of our estimator $\hat{\alpha}_j$. Assumptions are of standard nature in marker dependent hazard papers and they can be verified for the local constant estimators we are interested in, see in particular Nielsen and Linton (1995), Nielsen (1998) and Linton et al. (2003) for related arguments. However, the conditions are formulated more general and they are not restricted to the local constant smoothers. They are not even tight to kernel smoothers. Any smoother could be used as long as it obeys the structure of being a ratio of a smoothed occurrence and a smoothed exposure.

5 Simulation study

In this section we present detailed simulations of the smooth backfitter. The Supplementary Material contains additional simulation results for the setting discussed in Honda (2005) and Lin et al. (2016). In these latter settings, the performance of the smooth backfitter is similar to the estimator of Lin et al. (2016). And both estimators outperform the estimators considered in Honda (2005).

In the simulation study below, and with additional results in The Supplementary Material, we compare our estimator with the estimator of Lin et al. (2016). The models of these simulations contain high-dimensional and correlated covariates and in particular, we will show that our estimator – in contrast to Lin et al. (2016) – works in high dimensions where the dimension of the covariates is of similar order as the sample size and also in cases with higher correlation between the covariates. To highlight the impact of increasing dimension we will consider the dimensions $d = 2$ and $d = 9$. Further results for dimensions $d = 30$ and $d = 99$ can be found in the Supplementary Material. The low dimensional setting, $d = 2$, with uncorrelated covariates is similar to the setting of Honda (2005) and Lin et al. (2016), and the difference between our estimator and the estimator of Lin et al. (2016) are indeed marginal in this case. However, below and in the Supplementary Material we show that this changes drastically with increasing dimension and/or correlation.

5.1 The setting

Since the estimator of Lin et al. (2016) is based on a partial likelihood approach, it does not estimate the baseline hazard, α_0 . We will consider the sub-model

$$\alpha(x) = \prod_{k=0}^d \alpha_k(x_k) = \exp \left\{ \sum_{k=1}^d \eta_k(x_k) \right\},$$

i.e., we assume a constant baseline hazard, $\alpha_0 \equiv 1$. More specifically, we assume that the survival times T_i follow an exponential distribution with parameter value $\alpha(X_i)$, ($i = 1, \dots, n$). We add right censoring with censoring variables C_i that follow an exponential distribution with parameter $\frac{4}{7}\alpha(X_i)$, ($i = 1, \dots, n$). We will compare the estimators for $\eta_k, k = 1, \dots, d$. Our proposed estimator is derived as $\hat{\eta}_k^{SBF} = \log(\hat{\alpha}_k)$ and we compare it to, $\hat{\eta}_k^{\text{Lin et al.}}$, proposed in Lin et al. (2016).

We used the following two models:

$$\begin{aligned} \text{Model 1: } \eta_k(z_k) &= \begin{cases} -z_k & \text{if } k \text{ is odd,} \\ 2z_k & \text{if } k \text{ is even.} \end{cases} \\ \text{Model 2: } \eta_k(z_k) &= \begin{cases} 2 \sin(\pi z_k) & \text{if } k \text{ is odd,} \\ 2z_k & \text{if } k \text{ is even.} \end{cases} \end{aligned}$$

The covariates (Z_{i1}, \dots, Z_{id}) are generated as follows. We first simulate $(\tilde{Z}_{i1}, \dots, \tilde{Z}_{id})$ from a d -dimensional multi-normal distribution with mean equal 0 and $\text{Corr}(Z_{ij}, Z_{il}) = \rho$ if $j \neq l$, else 1. Afterwards we set

$$Z_{ik} = 2.5\pi^{-1} \arctan(\tilde{Z}_{ik}).$$

This has been independently repeated for every individual $i = 1, \dots, n$. After trying several bandwidths, if not said otherwise, we present the results for a bandwidth $b = 0.3$ for both estimators in every model. As kernel function k , we used the Epanechnikov kernel. Performance is measured via the integrated squared error evaluated at the observed points:

$$\begin{aligned} ISE_k &= n_{obs}^{-1} \sum_{i_{obs}} (\eta_k(Z_{i_{obs}k}) - \hat{\eta}_k(Z_{i_{obs}k}))^2, \\ ISE_{odd} &= \{ISE_k | k = odd\}, \quad ISE_{even} = \{ISE_k | k = even\}, \end{aligned}$$

where i_{obs} runs over all observed individuals and $n_{obs} < n$ is the number of observed individuals. The next two subsections discuss the outcomes of the simulations for $d = 2$ and $d = 9$.

5.2 Dimension $d = 2$

In low dimensions both estimators perform satisfactorily. Already in dimension $d = 2$, for Model 1, it occurred that the algorithm of Lin et al. (2016) stopped before the final calculation of the estimator. This happened for three simulation samples out of 1200 (6 settings \times 200 samples each) runs. The algorithm stopped at a step where a matrix has to be inverted that is nearly singular. In contrast, our estimator does not need to invert matrices and we did not have any singularity or convergence issues for our estimator. Performance-wise, we refer to Figure 2 displaying boxplots of the integrated squared errors of both estimators. The two estimators perform similar with a small advantage towards our smooth backfitting estimator. The smooth backfitting estimator performs especially better for the smaller sample size $n = 200$. While Lin et al. (2016) performed better in Model 2 with no correlation, the performance of the smooth backfitting estimator seems more stable when correlation is added. Figure 1 shows the 200 sample estimates of the first component α_1 of Model 2 with $\rho = 0.8$. The estimator of Lin et al. (2016) struggles especially at the boundaries and this is more pronounced with a small bandwidth (left panel). If bandwidth is increased (right panel), the estimate of Lin et al. (2016) seems over-smoothed and it is not able to replicate the full magnitude of the local extrema at -0.5 and 0.5 .

5.3 Dimension $d = 9$

When the dimension d is increased to 9, the estimator of Lin et al. (2016) breaks down considerably more often than in the case $d = 2$, i.e., in 59 (4+5+48+1+1 out of 1200) cases in Model 1 and 9 times in Model 2; see Table 1. Note that in the more extreme cases of $d = 99$, provided in the Supplementary Material, nearly all simulations of Lin et al. (2016) (780 and 607 out of 800 for Model 1 and Model 2, respectively) broke down. In contrast, our estimator converged in all cases considered. Performance-wise we refer to Figure 4

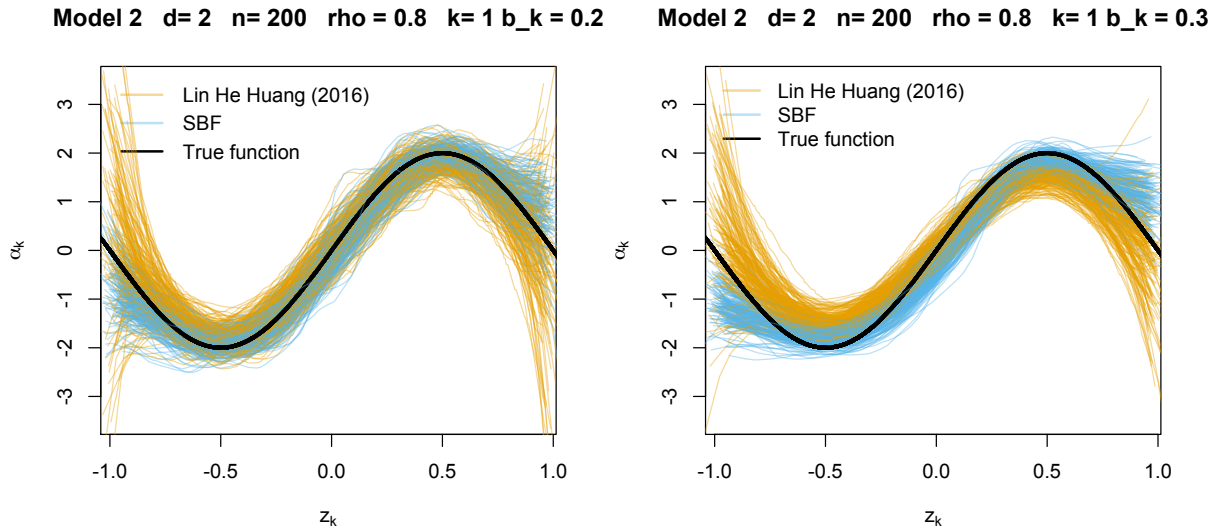


Figure 1: Estimates of α_1 from 200 simulations. Left panel uses a bandwidth of 0.2 and right panel a bandwidth of 0.3.

displaying boxplots of the integrated squared errors of both estimators. We see that for $d = 9$ the smooth backfitter performs better in every setting. The better performance is more pronounced when more correlation is present. Figure 3 shows 200 sample estimates of the first component α_1 of Model 2 with $\rho = 0.8$. The results are similar as in the case $d = 2$, but now more pronounced: The estimator of Lin et al. (2016) struggles at the boundaries and if bandwidth is increased (right panel), the estimate of Lin et al. (2016) seems too smooth and is not able to replicate to full magnitude of the local extrema at -0.5 and 0.5 .

6 In-sample forecasting of outstanding loss liabilities

The so-called chain ladder method is a popular approach to estimate outstanding liabilities. It started off as a deterministic algorithm, and it is used today for almost every single insurance policy over the world in the business of non-life insurance. In many developed

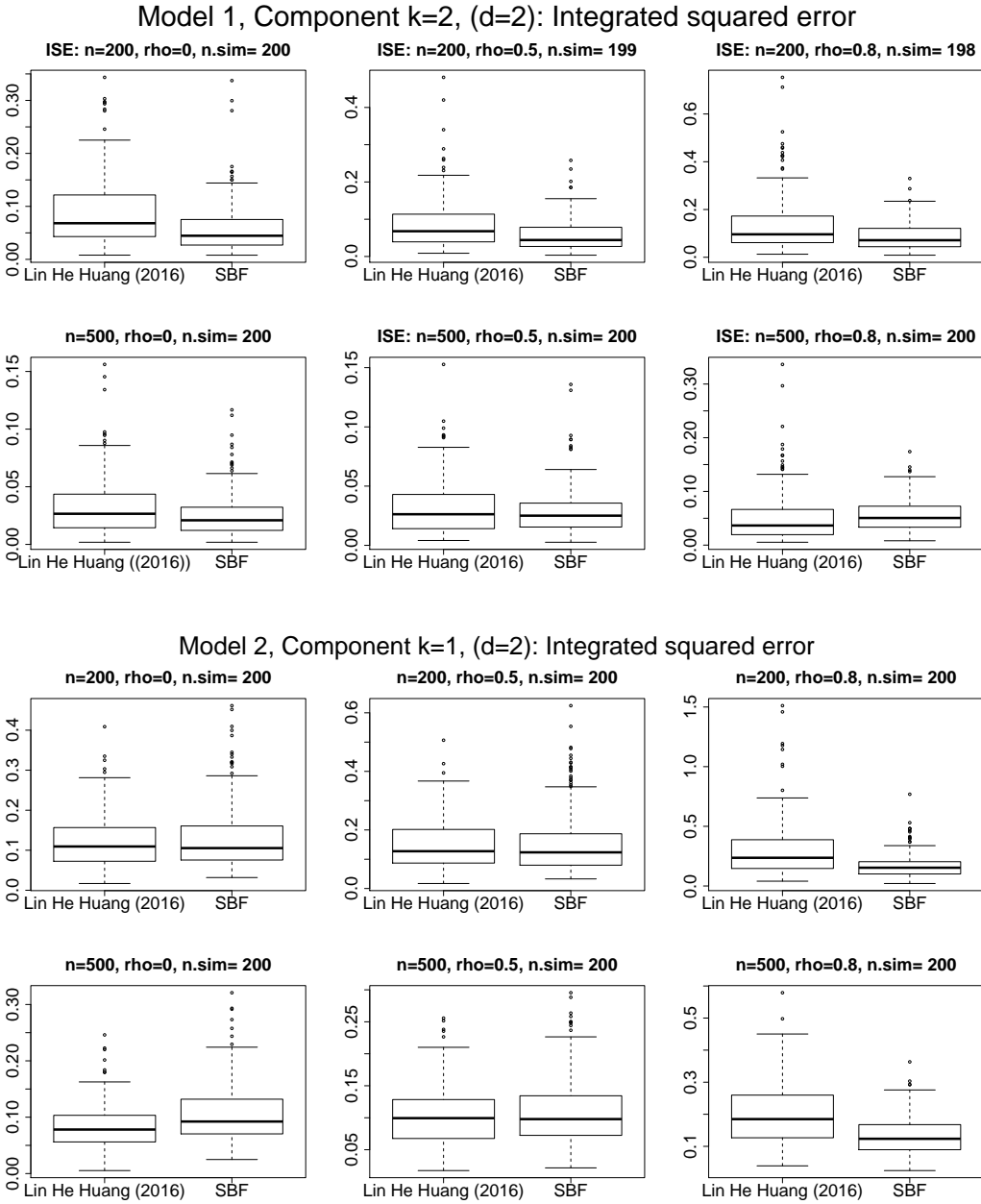


Figure 2: Boxplots of the integrated squared errors. Simulations are taken out where the algorithm for the calculation of the estimator in Lin et al. (2016) stopped without calculation of all values of the estimator. The value $n.sim$ is the number of the remaining simulations, i.e., 200 minus number of break downs.

Number of breakdowns in Lin et al. (2016) for $d = 9$ (out of 200 simulations)						
	Model 1			Model 2		
	$\rho = 0$	$\rho = 0.5$	$\rho = 0.8$	$\rho = 0$	$\rho = 0.5$	$\rho = 0.8$
n=200	4	5	48	0	0	9
n=500	0	1	1	0	0	0

Table 1: Number of breakdowns in the algorithm of Lin et al. (2016) out of 200 simulations for dimension $d = 9$.

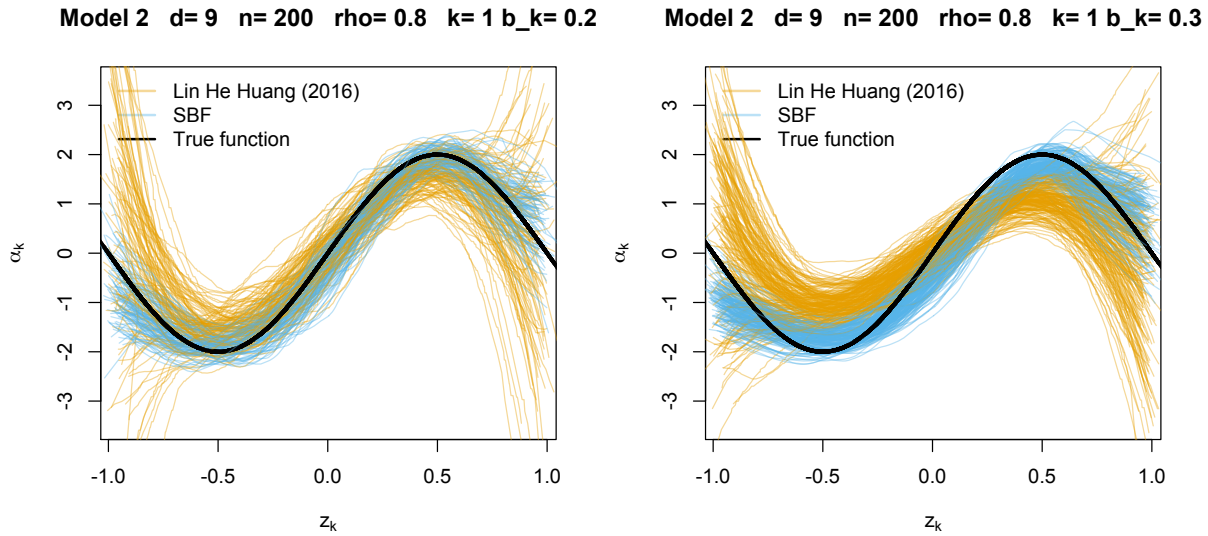


Figure 3: Estimates of α_1 from 200 simulations. Left panel uses a bandwidth of 0.2 and right panel a bandwidth of 0.3.

countries, the non-life insurance industry has revenues amounting to around 5%. It is therefore comparable to - but smaller than - the banking industry. In every single product sold, the chain ladder method (because actuaries hardly use other methods) comes in, estimating the outstanding liabilities that eventually aggregate to the reserve - the single biggest number of most non-life insurers balance sheets. The insurers liabilities often amount to many times the underlying value of the company. In Europe alone those outstanding liabilities are

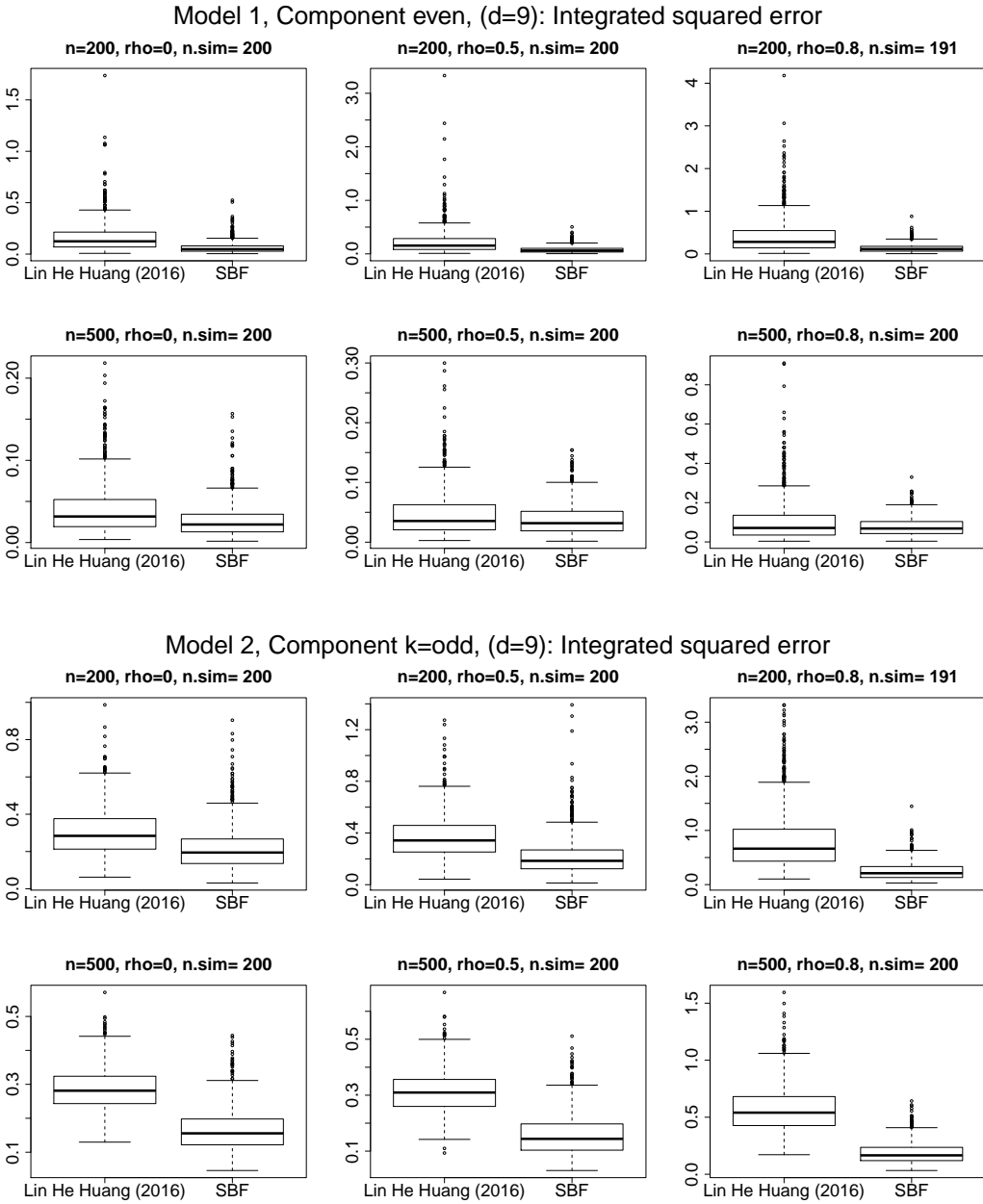


Figure 4: Boxplots of the integrated squared errors. Simulations are taken out where the algorithm for the calculation of the estimator in Lin et al. (2016) stopped without calculation of all values of the estimator. The value $n.sim$ is the number of the remaining simulations, i.e., 200 minus number of break downs.

estimated to accumulate to around €1trn. It is therefore of obvious importance that this estimate is not too far from the best possible estimate. We describe in this section how the methodology introduced in this paper can be applied to provide a solution to this challenging problem.

We analyze reported claims from a motor business line in Cyprus. The same data set has been used by Hiabu et al. (2016) and it consists of the number of claims reported between 2004 and 2013. During these 10 years (3654 days), $n = 58180$ claims were reported. The data are given as $\{(T_1, Z_1), \dots, (T_n, Z_n)\}$, where Z_i denotes the underwriting date of claim i , and T_i the time between underwriting date and the date of report of a claim in days, also called reporting delay. Hence, in the notation of the previous sections, the covariate underwriting date, $Z(t) = Z$, does not depend on time and has dimension $d = 1$. The data exist on a triangle, with $T_i + Z_i \leq 31 \text{ December } 2013 = R_0$, which is a subset of the full support $\mathcal{R} = [0, R_0]^2$ ($0 = 1 \text{ January } 2004$). The aim is to forecast the number of future claims from contracts written in the past which have not been reported yet. Figure 5 shows the observed data that lie on a triangle, while the forecasts are required on the triangle that added to the first completes a square. Here it is implicitly assumed that the maximum reporting delay of a claim is 10 years. Actuaries call this assumption that the triangle is fully run off. In our data set, this is a reasonable assumption looking at Figure 5.

The classical chain ladder method is able to provide a simple solution to the above problem. Recently, Martínez-Miranda et al. (2013) have pointed out that this method can be viewed as a multiplicative density method: the original, un-truncated random variable (T, Z) having density $f(t, z) = f_1(t)f_2(z)$; and the authors suggested to embed the method in a more standard mathematical statistical vocabulary to engage mathematical statisticians in future developments. In particular, Martínez-Miranda et al. (2013) showed that one could consider the traditional chain ladder estimator as a multiplicative histogram in a continuous framework, and presented an alternative by projecting an unconstrained local linear density

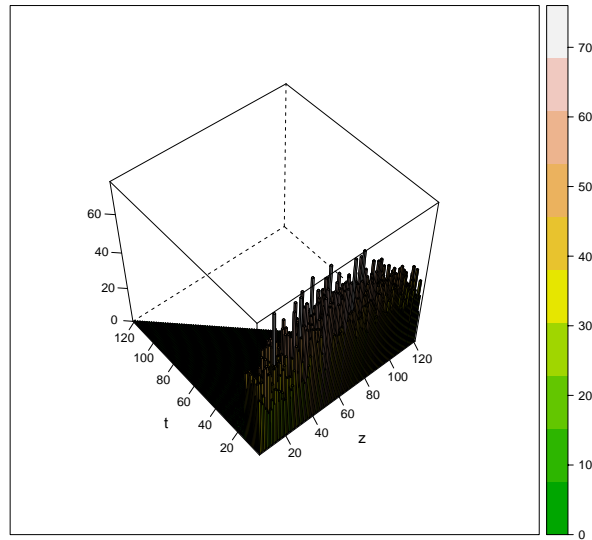


Figure 5: Histogram of claim numbers of a motor business line between 2004 and 2013. Axis z represents the underwriting time (in months) and axis t the reporting delay (in months).

down onto a multiplicative subspace. This approach was called continuous chain ladder and it has been further analyzed by Mammen et al. (2015); Lee et al. (2015, 2017), providing full asymptotic theory of the underlying density components. A related approach by Hiabu et al. (2016); Hiabu (2017) proposes to transform the two-dimensional multiplicative continuous chain ladder problem to two one-dimensional continuous hazard estimation problems via an elegant time-reverting trick. The application considered in this paper generalizes the most important of these reversed hazards to a two-dimensional multiplicatively structured hazard. In this way the continuous chain ladder is improved and generalized allowing more flexibility for the estimation of outstanding liabilities in the insurance business.

In Hiabu et al. (2016) it is assumed that T and Z are independent, which means that the underwriting date of a claim has no effect on the reporting delay. We are not going to impose such a strong restriction. In order to discuss the independence assumption, consider Figure 6. The points in the plots are derived by first transforming the data into a triangle

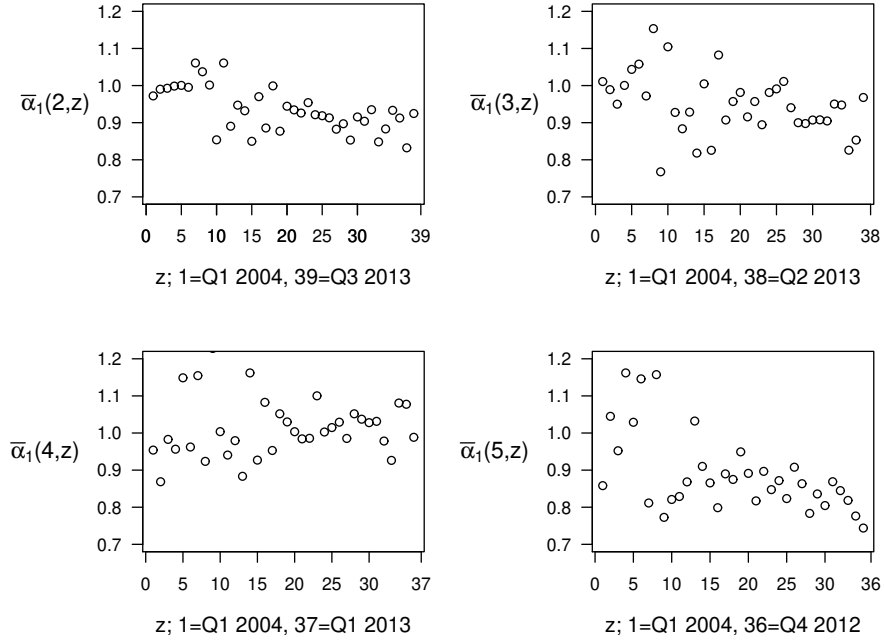


Figure 6: Scaled quarterly hazard rates of the first four development quarters.

with dimension 3654×3654 ,

$$\mathcal{N}_{t,z} = \sum_{i=1}^n I(T_i = t, Z_i = z), \quad (t, z) \in \{1, 2, \dots, 3654\}^2, t + z \leq 3654$$

and then aggregating the data into a quarterly triangle, $(\mathcal{N}_{t,z}^Q)$, with dimension 40×40 , see also Hiabu (2017). Then, for $t = 2, \dots, 5$, one derives the quarterly hazard rate as ratio of occurrence and exposure, $\bar{\alpha}(t, z) = \mathcal{N}_{t,z}^Q / \sum_{l=1}^z \mathcal{N}_{t,l}^Q$. These values are then scaled by an eye-picked norming factor, $\bar{\alpha}_0(t), t = 2, \dots, 5$, letting $\bar{\alpha}(t, z)$ start at around 1 as a function of z with fixed t . The final values, $\bar{\alpha}_1(t, z) = \bar{\alpha}_0(t) \bar{\alpha}(t, z)$, are displayed in Figure 6. We only show plots for $t \leq 5$ since almost all claims are reported after five quarters.

If the independence assumption of Hiabu et al. (2016) is satisfied, the points should lie around a horizontal line in each plot. If the multiplicative hazard assumption of this paper is

satisfied, then any smooth shape is allowed, but all four graphs must be equal after correction for noise. This is because under the model which will be defined below, the graphs, $\bar{\alpha}_1(\cdot, \cdot)$, with the first component fixed, mimic a quarterly version of α_1 .

Inspecting the four plots, one can argue to see a negative drift of similar magnitude in each graph, the values decaying from around 1 to 0.8. This indicates that the approach of this paper should give a better fit to the data compared to the model of Hiabu et al. (2016).

From this discussion we now continue with embedding our observations in the proportional hazard framework. Afterwards we will show how the hazard estimate can be used to forecast the number of outstanding claims. First note that we cannot apply the approach of this paper directly, since in this application we only observe T if $T \leq R_0 - Z$, which is a right truncation. Analogue to Hiabu et al. (2016), we transform the random variable T to $T^R = R_0 - T$. This has the result that the right truncation truncation becomes left truncation, $T^R \geq Z$. Thus we consider the random variable T^R as our variable of interest. With the notation considered in Section 2.1, we now have $T = T^R, d = 1, Z(t) = Z, \delta = 1, \mathcal{I} = \{(t^R, z) \in \mathcal{R} | 0 \leq z \leq t^R\}$. We conclude that the counting process $N_i(t^R) = \mathbb{1}\{T_i^R \leq t^R\}$, satisfies Aalen's multiplicative intensity model with respect to the filtration given in Section 2.1 and

$$\alpha_z(t^R) = \alpha(t^R, z) = \lim_{h \downarrow 0} h^{-1} \Pr\{T^R \in [t^R, t^R + h) | T^R \geq t^R, Z = z\},$$

$$Y_i(t^R) = \mathbb{1}\{(t^R, Z_i) \in \mathcal{I}, t^R \leq T_i^{R,*}\}.$$

In Section 3.1 we suggested a local constant estimator as pilot. In this application we prefer a local linear estimator because we anticipate high mass at the boundaries. The local linear estimator (Nielsen, 1998) has an automated boundary correction. We estimate the unstructured hazard as ratios of occurrence and exposure from a local linear estimation

(Gámiz et al., 2013):

$$\begin{aligned}\widehat{O}^{LL}(x) &= n^{-1} \sum_{i=1}^n \int \{1 - (x - X_i(s))D(x)^{-1}c_1(x)\} K_b(x - X_i(s))dN_i(s), \\ \widehat{E}^{LL}(x) &= n^{-1} \sum_{i=1}^n \int \{1 - (x - X_i(s))D(x)^{-1}c_1(x)\} K_b(x - X_i(s))Y_i(s)ds,\end{aligned}$$

where the components of the $(d + 1)$ - dimensional vector c_1 are

$$c_{1j}(x) = n^{-1} \sum_{i=1}^n \int K_b(x - X_i(s))(x_j - X_{ij}(s))Y_i(s)ds, \quad j = 0, \dots, d,$$

and the entries (d_{jk}) of the $(d + 1) \times (d + 1)$ - dimensional matrix $D(x)$ are given by

$$d_{jk}(x) = n^{-1} \sum_{i=1}^n \int K_b(x - X_i(s))(x_j - X_{ij}(s))(x_k - X_{ik}(s))Y_i(s)ds.$$

Note that we have $\mathcal{X} = \mathcal{I}$. The components of the multiplicative conditional hazard are then computed as in (3.5). These estimators require the choice of the bandwidth parameter, which was assumed to be scalar in order to simplify the notation in this paper. In this application we generalize this restriction allowing for different smoothing levels in each dimension, namely reporting delay and underwriting time. The bandwidth parameter is then a vector $b = (b_0, b_1)$ and we estimate it using cross-validation, see further details in the Supplementary Material. To alleviate the computational burden of cross-validation we aggregated the data triangle $\mathcal{N}_{t,z}$ considering bins of two days when applying a discrete version of the estimators described in the Supplementary Material. After several trials we run the cross-validation minimization over $b_0 \in \{1300, 1400, 1500, 1600, 1700, 1800\}$ and $b_1 \in \{2, 3, 4, 5\}$. The cross-validated bandwidth components were $b_0 = 1600$ and $b_1 = 3$ (unit=2 days).

The result of the estimation procedure is given in Figure 7 which displays the estimated components of the multiplicatively structured hazard estimator. The function α_2 which

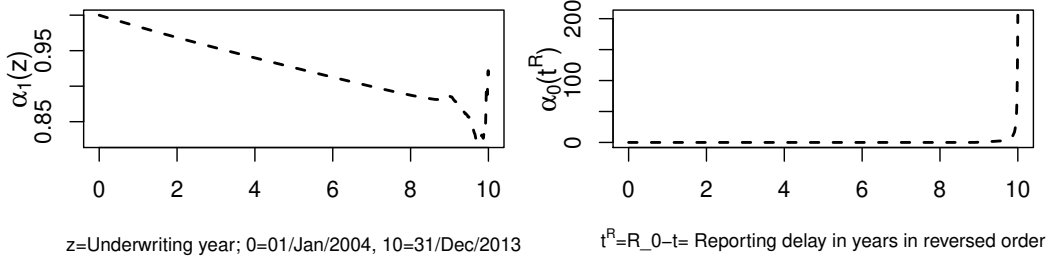


Figure 7: The estimated multiplicative hazard components .

captures the underwriting date effect, seems, up to a possible boundary effect, linear. This suggests that a semiparametric approach with nonparametric baseline hazard and linear covariate effect might be suitable. While we do not investigate this point further in our data illustration, this particular case illustrates nicely how our nonparametric approach could be employed for model selection.

Finally the total number of outstanding claims, i.e. the reserve, can be estimated as

$$\text{Reserve} = \sum_{i=1}^n \frac{\int_{R_0-Z_i}^{R_0} \widehat{f}_{Z_i}(t) dt}{\int_0^{R_0-Z_i} \widehat{f}_{Z_i}(t) dt}, \quad \widehat{f}_z(t) = \widehat{\alpha}_0(R_0 - t) \widehat{\alpha}_1(z) \exp \left\{ - \int_0^{R_0-t} \widehat{\alpha}_0(s) \widehat{\alpha}_1(z) ds \right\}.$$

Note that $\widehat{f}_z(t)$ is an estimator of the conditional density of the survival time T . The reserve can be also decomposed further to provide the 'cash flow' of the next periods. If the future is divided into M periods, each of them with length $\delta = R_0/M$, then the amount of claims forthcoming in the a th ($a = 1, 2, \dots, M$) period can be estimated by

$$\text{Reserve}_P(a) = \sum_{i=1}^n \frac{\int_{(R_0-Z_i+a\delta-1)\wedge R_0}^{(R_0-Z_i+a\delta)\wedge R_0} \widehat{f}_{Z_i}(t) dt}{\int_0^{R_0-Z_i} \widehat{f}_{Z_i}(t) dt}.$$

Table 2 shows the estimated number of of outstanding claims for future quarters. We compare the approach of this paper with the results derived by Hiabu et al. (2016) and the traditional chain ladder method. The two latter approaches have in common that they

Table 2: Number of outstanding claims for future quarters; 1 = 2014 Q1, . . . , 39 = 2022 Q3. The backfitting approach in this paper (SBF) is compared with the chain ladder method (CLM) and the approach in Hiabu et al. (2016).

Future quarter	1	2	3	4	5	6	7	8	9	10	11	12 – 39	Tot.
Hiabu et al. (2016)	970	684	422	166	14	5	3	2	1	1	1	0	2270
CLM	948	651	387	148	12	5	3	2	1	1	1	0	2160
SBF	872	621	400	130	53	7	4	3	2	1	1	1	2193

assume independence between underwriting date, Z , and reporting delay, T . We see that while all approaches estimate a similar total number of outstanding claims (reserve), those two approaches have distributions over the quarters that are very different from the results obtained by the method proposed in this paper. It seems that the violation of the independence assumption has not a big influence on the reserve, since it balances the different development patterns arising from different periods out. However, the problem becomes quite serious if one is interested in more detailed estimates like the cash flow.

Appendix

A Asymptotic properties of the smooth backfitter of multiplicative hazards

The estimator $\hat{\alpha}_j$ is defined as solution of a nonlinear operator equation. We are going to approximate this equation by a linear equation that can be interpreted as equation that arises in nonparametric additive regression models, and then show that the solution of the linear equation approximates $\hat{\alpha}_j$. The linear equation and its solution is well understood from the theory of additive models. This will be our essential step to arrive at an asymptotic understanding of our estimator $\hat{\alpha}_j$. Assumptions [B1]-[B7] below are of standard nature in marker dependent hazard papers and can be verified for the local constant estimators we are interested, see in particular Nielsen and Linton (1995), Nielsen (1998) and Linton et al. (2003) for related calculations. However, one should notice that the conditions are not restricted to the local constant smoothers. They are not even tight to kernel smoothers. Any smoother could be used as long as it obeys the structure of being a ratio of a smoothed occurrence and a smoothed exposure.

For our main theorem we make the following assumptions. We hereby do not make assumptions on the full support \mathcal{R} but only on a subset $\mathcal{X} \subseteq \mathcal{R}$. We will make use of the following notations: \mathcal{X}_{x_k} denotes the set

$\{(x_0, \dots, x_{k-1}, x_{k+1}, \dots, x_d) \mid (x_0, \dots, x_d) \in \mathcal{X}\}$, and

$x_{-k} = (x_0, \dots, x_{k-1}, x_{k+1}, \dots, x_d)$ and \mathcal{X}_{x_j, x_k} denotes the set $\{(x_l : l \in \{0, \dots, d\} \setminus \{j, k\}) \mid (x_0, \dots, x_d) \in \mathcal{X}\}$. Furthermore, we define $\mathcal{X}_k = \{x_k \mid (x_0, \dots, x_d) \in \mathcal{X} \text{ for some values of } (x_l : l \neq k)\}$,

$\mathcal{X}_{j,k} = \{(x_j, x_k) \mid (x_0, \dots, x_d) \in \mathcal{X} \text{ for some values of } (x_l : l \notin \{j, k\})\}$, and $\mathcal{X}_{j(x_k)} =$

$\{x_j \mid (x_0, \dots, x_d) \in \mathcal{X} \text{ for some values of } (x_l : l \notin \{j, k\})\}$.

A1 The function $E(x)$ is two times continuously differentiable for $x \in \mathcal{X}$ and $\inf_{x \in \mathcal{X}} E(x) > 0$.

A2 The hazard α is two times continuously differentiable for $x \in \mathcal{X}$ and $\inf_{x \in \mathcal{X}} \alpha(x) > 0$.

A3 The kernel K has compact support which is without loss of generality supposed to be $[-1, 1]$. Furthermore it is symmetric and continuous.

A4 It holds that $nb^5 \rightarrow c_b$ for a constant $0 < c_b < \infty$ as $n \rightarrow \infty$.

A5 It holds that

$$\int_{\mathcal{X}_{j,k}} \frac{1}{O_j(x_j)O_k(x_k)} dx_j dx_k < \infty$$

for $j, k = 0, \dots, d, j \neq k$, where $O_j(x_j) = \int O(x) dx_{-j}$ and $O(x) = \alpha^* \prod_{j=0}^d \alpha_j(x_j)E(x)$.

A6 It holds that the two-dimensional marginal occurrences $O_{j,k}(x_j, x_k) = \int O(x) dx_{-(j,k)}$ are bounded from above and bounded away from 0.

A7 For some $\delta > 0$ it holds that for $j, k = 0, \dots, d, j \neq k$

$$\begin{aligned} \int_{\mathcal{X}_{j,k}} \frac{1}{O_j^{1+\delta}(x_j)O_k(x_k)} dx_j dx_k &< \infty, \\ \sup_{x_k \in \mathcal{X}_k} \int_{\mathcal{X}_{j(x_k)}} \frac{1}{O_j^{1-\delta}(x_j)O_k(x_k)} dx_j &< \infty, \\ \sup_{x_k \in \mathcal{X}_k} \int_{\mathcal{X}_{j(x_k)}} \frac{1}{O_j^{1/2}(x_j)O_k^{1/2}(x_k)} dx_j &< \infty. \end{aligned}$$

Note that assumptions [A1]-[A4] are standard in kernel smoothing theory. In Assumptions [A5] and [A6] we only assume that the two-dimensional marginal occurrences of O are bounded from above and bounded away from 0, but we do not make the assumption that the one-dimensional marginal occurrences have this property. This allows that the support of a two-dimensional marginal density O_{jk} has a triangular shape

$\{(x_j, x_k) : x_j + x_k \leq c; x_j, x_k \geq 0\}$ for some constant $c > 0$. This can be easily seen. Suppose for simplicity that O_{jk} is the uniform density on the triangle. Then $O_j(x_j) = 2c^{-2}(c - x_j)_+$ and $O_k(x_k) = 2c^{-2}(c - x_k)_+$ and we have

$$\int \frac{1}{O_j(x_j)O_k(x_k)} dx_j dx_k = \int_{x_j+x_k \leq c; x_j, x_k \geq 0} \frac{2}{c^2} \frac{1}{(c-x_j)(c-x_k)} dx_j dx_k = \frac{\pi^2}{3c^2} < \infty.$$

Thus, our assumption [A5] on one-dimensional marginals is fulfilled. One can easily verify that also [A7] holds for this example. This discussion can be extended to other shapes of two-dimensional marginals that differ from rectangular supports. Note also that [A5] and [A7] trivially hold if the one-dimensional marginal O_j are bounded away from zero.

The estimators $\hat{\alpha}_0, \dots, \hat{\alpha}_d$ can be rewritten as solutions of

$$\int_{\mathcal{X}_{x_k}} \hat{O}(x) dx_{-k} - \int_{\mathcal{X}_{x_k}} \hat{\alpha}^* \prod_{j=0}^d \hat{\alpha}_j(x_j) \hat{E}(x) dx_{-k} = 0, \quad k = 0, \dots, d.$$

Since, $\int_{\mathcal{X}_{x_k}} O(x) dx_{-k} - \int_{\mathcal{X}_{x_k}} \alpha^* \prod_{j=0}^d \alpha_j(x_j) E(x) dx_{-k} = 0$, the difference of those two zero-terms is zero as well, and we have

$$\begin{aligned} 0 &= \hat{\Delta}_k(x_k) - \int_{\mathcal{X}_{x_k}} \left\{ \hat{\alpha}^* \prod_{j=0}^d \hat{\alpha}_j(x_j) - \alpha^* \prod_{j=0}^d \alpha_j(x_j) \right\} \hat{E}(x) dx_{-k} \\ &= \hat{\Delta}_k(x_k) - \int_{\mathcal{X}_{x_k}} \left[(1 + \hat{\delta}^*) \prod_{j=0}^d \{1 + \hat{\delta}_j(x_j)\} - 1 \right] \alpha^* \prod_{j=0}^d \alpha_j(x_j) \hat{E}(x) dx_{-k}, \end{aligned} \quad (\text{A.1})$$

where

$$\begin{aligned}\widehat{\Delta}_k(x_k) &= \int_{\mathcal{X}_{x_k}} \left\{ \widehat{O}(x) - O(x) \right\} dx_{-k} - \int_{\mathcal{X}_{x_k}} \alpha^* \prod_{j=0}^d \alpha_j(x_j) \{ \widehat{E}(x) - E(x) \} dx_{-k}, \\ \widehat{\delta}_j(x_j) &= \frac{\widehat{\alpha}_j(x_j) - \alpha_j(x_j)}{\alpha_j(x_j)}, \\ \widehat{\delta}^* &= \frac{\widehat{\alpha}^* - \alpha^*}{\alpha^*}.\end{aligned}$$

Note that $\widehat{\delta}$ is defined as a root of a non-linear operator. Motivated by (A.1), we define an approximation, $\bar{\delta}^*$ and $\bar{\delta}_j(x_j)$ ($0 \leq j \leq d$), as solution of the linear equation

$$\int_{\mathcal{X}_{x_k}} \left[\bar{\delta}^* + \sum_{j=0}^d \bar{\delta}_j(x_j) \right] \alpha^* \prod_{j=0}^d \alpha_j(x_j) \widehat{E}(x) dx_{-k} = \widehat{\Delta}_k(x_k) \quad (\text{A.2})$$

under the constraint $\int \bar{\delta}_k(x_k) \omega_k(x_k) dx_k = 0$ where

$$\omega_k(x_k) = \int \prod_{j=0}^d \alpha_j(x_j) \widehat{E}(x) dx_{-k}.$$

This is equal to the constraint (3.4) in the main paper for the choice $w_k(x_k) = \int \prod_{j=0}^d \alpha_j(x_j) \widehat{E}(x) dx_{-k} / (\alpha_k(x_k) \int \prod_{j=0}^d \alpha_j(x_j) \widehat{E}(x) dx)$. Under this constraint one has that

$$\bar{\delta}^* = \frac{\int_{\mathcal{X}} \left\{ \widehat{O}(x) - O(x) \right\} dx - \int_{\mathcal{X}} \alpha^* \prod_{j=0}^d \alpha_j(x_j) \{ \widehat{E}(x) - E(x) \} dx}{\int_{\mathcal{X}} \alpha^* \prod_{j=0}^d \alpha_j(x_j) \widehat{E}(x) dx}.$$

Note that the norming of the constraint cannot be used in practice because α is unknown but it will simplify the theoretical discussion and the results can be carried over to feasible weighting.

Equation (A.2) can be rewritten as an integral equation of the second kind

$$\bar{\delta}_k(x_k) + \sum_{j \neq k} \int_{\mathcal{X}_j(x_k)} \hat{\pi}_{k,j}(x_k, x_j) \bar{\delta}_j(x_j) dx_j = \hat{\mu}_k(x_k) - \bar{\delta}^*,$$

with

$$\begin{aligned} \tilde{O}(x) &= \alpha^* \prod_{j=0}^d \alpha_j(x_j) \hat{E}(x), \\ \tilde{O}_{j,k}(x_j, x_k) &= \int \tilde{O}(x) dx_{-(j,k)}, \\ \tilde{O}_k(x_k) &= \int \tilde{O}(x) dx_{-k}, \\ \hat{\pi}_{k,j}(x_k, x_j) &= \frac{\tilde{O}_{j,k}(x_j, x_k)}{\tilde{O}_k(x_k)}, \\ \hat{\mu}_k(x_k) &= \frac{\hat{\Delta}_k(x_k)}{\tilde{O}_k(x_k)}. \end{aligned}$$

Note that all these functions depend on n . The integral equation can also be simply written as $\bar{\delta} + \hat{\pi} \bar{\delta} = \hat{\mu} - \bar{\delta}^*$ with $\bar{\delta} = (\bar{\delta}_0, \dots, \bar{\delta}_d)^\top$, where $\hat{\pi}$ is the integral operator with kernel $\hat{\pi}_{k,j}$. We will show that $\bar{\delta}$ approximates $\hat{\delta}$. Before we come to this point we state a proposition that gives the asymptotics for $\bar{\delta}$.

For the next results we need some conditions on the estimators \hat{E} and \hat{O} . We decompose $\hat{\mu}_k$ into three terms, $\hat{\mu}_k = \hat{\mu}_k^A + \hat{\mu}_k^B + \hat{\mu}_k^C$, which depend on n . For some deterministic functions

$O^*(x)$ and $E^*(x)$ these terms are defined as:

$$\begin{aligned}\widehat{\mu}_k^A(x_k) &= \frac{-\int_{\mathcal{X}_{x_k}} \alpha^* \prod_{j=0}^d \alpha_j(x_j) \left\{ \widehat{E}(x) - E^*(x) \right\} dx_{-k} + \int_{\mathcal{X}_{x_k}} \left\{ \widehat{O}(x) - O^*(x) \right\} dx_{-k}}{\widetilde{O}_k(x_k)}, \\ \widehat{\mu}_k^B(x_k) &= \frac{-\int_{\mathcal{X}_{x_k}} \alpha^* \prod_{j=0}^d \alpha_j(x_j) \left\{ E^*(x) - E(x) \right\} dx_{-k} + \int_{\mathcal{X}_{x_k}} \left\{ O^*(x) - O(x) \right\} dx_{-k}}{O_k(x_k)}, \\ \widehat{\mu}_k^C(x_k) &= \left[\frac{O_k(x_k)}{\widetilde{O}_k(x_k)} - 1 \right] \widehat{\mu}_k^B(x_k).\end{aligned}$$

Note that $\widehat{\mu}_k^B$ are deterministic functions. Typical choices of $O^*(x)$ and $E^*(x)$ are the expectations of $\widehat{E}(x)$ and $\widehat{O}(x)$. Then $\widehat{\mu}_k^A(x_k)$ is the stochastic part of a one-dimensional smoother and $\widehat{\mu}_k^B(x_k)$ is its bias. Both terms are well understood and can be easily treated by standard smoothing theory. We now want to develop an asymptotic theory for the estimators $\hat{\alpha}_j$ where their asymptotic properties are described by the properties of $\widehat{\mu}_k^A(x_k)$ and $\widehat{\mu}_k^B(x_k)$. We use the following normings of these quantities: $\bar{\mu}_k^{*,r} = \int \widehat{\mu}_k^r(x_k) O_k(x_k) dx_k$ for $r \in \{A, B, C\}$ and $\bar{\mu}_k^{*,r,n} = \int \widehat{\mu}_k^r(x_k) \widetilde{O}_k(x_k) dx_k$ for $r \in \{A, B, C\}$.

We assume that with

$$\pi_{k,j}(x_k, x_j) = \frac{\int \prod_{l=0}^d \alpha_l(x_l) E(x) dx_{-(k,j)}}{\int \prod_{l=0}^d \alpha_l(x_l) E(x) dx_{-k}}$$

the following assumptions hold:

B1 It holds that $\int \widetilde{O}(x)^2 dx = O_P(1)$ and

$$\widetilde{O}_{j,k}(x_j, x_k) - O_{j,k}(x_j, x_k) = o_P((\log n)^{-1})$$

uniformly over $0 \leq j < k \leq d$ and x_j, x_k , where $O_{j,k}(x_j, x_k) = \int O(x) dx_{-(j,k)}$.

B2

$$\sup_{x_j} |O_j^{1/2}(x_j) \widehat{\mu}_j^A(x_j)| = o_P(n^{-1/5})$$

and

$$\sup_{x_j} |O_j^{1/2}(x_j) \widehat{\mu}_j^B(x_j)| = o_P(n^{-1/5})$$

for $0 \leq j \leq d$, where $O_j(x_j) = \int O(x) dx_{-j}$.

B3 For x_j with $O_j(x_j) > 0$ it holds that

$$n^{2/5} \widehat{\mu}_j^A(x_j) \rightarrow N(0, \sigma_j^2(x_j))$$

for $0 \leq j \leq d$ with some function $\sigma_j^2(x_j) > 0$.

B4

$$\int \widehat{\mu}_j^A(x_j)^2 O_j(x_j) dx_j = O_P(n^{-4/5})$$

and

$$\int \widehat{\mu}_j^B(x_j)^2 O_j(x_j) dx_j = O(n^{-4/5})$$

for $0 \leq j \leq d$.

B5 It holds that

$$\sup_{x_j \in \mathcal{X}_j} O_j^{1/2}(x_j) \int_{\mathcal{X}_k(x_j)} \frac{O_{j,k}(x_j, x_k)}{O_j(x_j)} \widehat{\mu}_k^A(x_k) dx_k = o_P(n^{-2/5} (\log n)^{-1}).$$

B6 It holds for $0 \leq j \leq d$ that

$$\begin{aligned} \sup_{x_j \in \mathcal{X}_j} \int_{x \in \mathcal{X}} \frac{1}{\prod_{k \in \{0, \dots, d\} \setminus \{j\}} O_k(x_k)^{1/2}} \tilde{O}(x) dx_{-j} &= O_P(1), \\ \sup_{x_j \in \mathcal{X}_j} \int_{x \in \mathcal{X}} \frac{1}{\prod_{k \in \{0, \dots, d\} \setminus \{j\}} O_k(x_k)^{1/2}} O(x) dx_{-j} &= O(1). \end{aligned}$$

B7 It holds that $\bar{\mu}^{*,B,n} - \bar{\mu}^{*,B} = o_p(n^{-2/5})$.

We shortly discuss these assumptions. Condition [B1] is a mild consistency assumption for a two-dimensional smoother. Also [B2] is a weak condition because in our setting one-dimensional smoothers are typically $O_P(n^{-2/5})$ -consistent. [B3] is a standard limit result for many one-dimensional smoothers and [B4] assumes rates for L_2 -norms of the stochastic part and the bias part of a nonparametric one-dimensional smoother that are standard under our smoothness assumptions. For the interpretation of [B5] note that the integral on the left hand side in the formula is a global average of $\hat{\mu}_k^A$. Because $\hat{\mu}_k^A$ is a local average this is a global weighted average of mean zero random variables. Thus one expects a $O_P(n^{-1/2})$ rate for the integral. For the supremum of the integrals one expects a $O_P((\log n)^{1/2} n^{-1/2})$ rate which is faster than the required rate. [B6] states a bound for the total number of occurrences. It can be easily verified under the assumption that the one dimensional marginals O_l are bounded from below. Furthermore, one can easily check it if the one-dimensional marginals O_l are bounded from below for $l \notin \{j, k\}$ and if the two-dimensional marginal $O_{j,k}$ has the properties discussed in the example after assumption [A7]. The following proposition states a stochastic expansion for $\bar{\delta}$.

Proposition 1. *Make the assumptions [A1]–[A7], [B1]–[B7]. Then the function $\bar{\delta} = (\bar{\delta}_0, \dots, \bar{\delta}_d)$, introduced in (A.2), exists and is uniquely defined, with probability tending to*

one. Moreover, it has the following expansion:

$$\|\bar{\delta} - \widehat{\mu}^A - (I - \pi)^{-1}(\widehat{\mu}^B - \bar{\mu}^{*,B})\|_{O,\infty} = o_p(n^{-2/5}),$$

where, for a function $f(x) = (f_0(x_0), \dots, f_d(x_d))^\top$, we define

$$\|f\|_{O,\infty} = \sup_{x \in \mathcal{X}} \max_{0 \leq j \leq d} |O_j^{1/2}(x_j) f_j(x_j)|.$$

Furthermore, the function $\pi : \mathcal{L} \rightarrow \mathcal{L}$ is defined as $\pi_k(f)(x_k) = \sum_{j \neq k} \int \pi_{kj}(x_k, x_j) f_j(x_j) dx_j$ for $f \in \mathcal{L} = \mathcal{L}_1 \times \dots \times \mathcal{L}_d$ with $\mathcal{L}_j = \{\delta_j : \mathcal{X}_j \rightarrow \mathbb{R} : \int_{\mathcal{X}_j} \delta_j^2(x_j) O_j(x_j) dx_j < \infty, \int_{\mathcal{X}_j} \delta_j(x_j) O_j(x_j) dx_j = 0\}$.

From the proposition we get as a corollary the asymptotic distribution of $\bar{\delta}_j(x_j)$.

Proposition 2. *Make the assumptions [A1]–[A7], [B1]–[B7]. Then for x_j ($0 \leq j \leq d$) with $O_j(x_j) > 0$ it holds that*

$$n^{2/5} \{\bar{\delta}_j(x_j) - [(I - \pi)^{-1}(\widehat{\mu}^B - \bar{\mu}^{*,B})]_j(x_j)\} \rightarrow N(0, \sigma_j^2(x_j)),$$

in distribution. Under the additional assumption $\widehat{\mu}_j^B(x_j) = O(n^{-2/5})$ we have that the bias $[(I - \pi)^{-1}(\widehat{\mu}^B - \bar{\delta}^{B,*})]_j(x_j)$ is of order $O(n^{-2/5})$.

The following theorem states that $\bar{\delta}$ is indeed a good approximation of the relative estimation error $\widehat{\delta}$.

Theorem 3. *Under assumptions [A1]–[A7], [B1]–[B7] it holds that with probability tending to one there exists a solution $\widehat{\delta}^*$ and $\widehat{\delta} = (\widehat{\delta}_0, \dots, \widehat{\delta}_d)$ that solves equation (A.1) with*

$$\begin{aligned} \|\widehat{\delta} - \bar{\delta}\|_{O,\infty} &= o_p(n^{-2/5}), \\ \widehat{\delta}^* - \bar{\delta}^* &= o_p(n^{-2/5}). \end{aligned}$$

For this solution we get that

$$n^{2/5}\{(\widehat{\alpha}_j - \alpha_j)(x_j) - \alpha_j(x_j)[(I - \pi)^{-1}(\widehat{\mu}^B - \bar{\mu}^{*,B})]_j(x_j)\} \rightarrow N(0, \alpha_j^2(x_j)\sigma_j^2(x_j)),$$

in distribution, for x_j ($0 \leq j \leq d$) with $O_j(x_j) > 0$.

B Proofs

B.1 Proof of Proposition 1

The proof of this proposition follows the lines of the proof of Theorem 1 in Mammen et al. (1999) but it needs some major modifications in the last steps of the proof because we have weaker assumptions than the ones assumed in the latter theorem. We outline that the first part of the proof in Mammen et al. (1999) also goes through under our weaker assumptions and we show how additional arguments can be used in the last part.

Note that under our assumptions [A5], [A6] we get that $\int O_{jk}(x_j, x_k)^2 O_j(x_j)^{-1} O_k(x_k)^{-1} dx_j dx_k < \infty$. As in Lemma 1 in Mammen et al. (1999) this implies that for some constants $c, C > 0$

$$c \max_{0 \leq j \leq d} \|\delta_j\| \leq \|\delta_0 + \dots + \delta_d\| \leq C \max_{0 \leq j \leq d} \|\delta_j\| \tag{B.1}$$

for $\delta_j \in \mathcal{L}_j$ where $\|\dots\|$ denotes the norm $\|m(x)\|^2 = \int m(x)^2 O(x) dx$. Furthermore, one gets that $\|T\| = \sup\{\|T(\delta_0 + \dots + \delta_d)\| : \delta_j \in \mathcal{L}_j \text{ with } \|\delta_0 + \dots + \delta_d\| < 1\} < 1$, where here T is

the operator $T = \Psi_d \cdot \dots \cdot \Psi_0$ with

$$\begin{aligned} \Psi_j(\delta^* + \delta_0 + \dots + \delta_d)(x) &= \delta^* + \delta_0(x_0) + \dots + \delta_{j-1}(x_{j-1}) \\ &\quad + \delta_j^*(x_j) + \delta_{j+1}(x_{j+1}) + \dots + \delta_d(x_d), \\ \delta_j^*(x_j) &= - \sum_{k \neq j} \int \delta_k(x_k) \pi_{j,k}(x_j, x_k) \, dx_k \end{aligned}$$

for $(\delta^*, \delta_0, \dots, \delta_d) \in \mathcal{L}$. Furthermore, note that for $j \neq k$ it holds that

$$\begin{aligned} \left\| \frac{\tilde{O}_j(x_j) - O_j(x_j)}{O_j(x_j)} \right\| &= o_P(1), \\ \int \left(\frac{\tilde{O}_{j,k}(x_j, x_k)}{O_j(x_j)O_k(x_k)} - \frac{O_{j,k}(x_j, x_k)}{O_j(x_j)O_k(x_k)} \right)^2 O_j(x_j)O_k(x_k) \, dx_j \, dx_k &= o_P(1), \\ \int \left(\frac{\tilde{O}_{j,k}(x_j, x_k)}{\tilde{O}_j(x_j)O_k(x_k)} - \frac{O_{j,k}(x_j, x_k)}{O_j(x_j)O_k(x_k)} \right)^2 O_j(x_j)O_k(x_k) \, dx_j \, dx_k &= o_P(1). \end{aligned}$$

These equations follow from [A5], [A6] and [B1]. To see this note that [A6] and [B1] imply that, uniformly for x_j, x_k it holds that $\tilde{O}_{j,k}(x_j, x_k) - O_{j,k}(x_j, x_k) = o_P((\log n)^{-1})O_{j,k}(x_j, x_k)$.

This gives that

$$[\tilde{O}_j(x_j)/O_j(x_j)] - 1 = o_P((\log n)^{-1}), \quad (\text{B.2})$$

uniformly for $x_j \in \mathcal{X}_j$ and $0 \leq j \leq d$. Together with [A5] and [B1], this implies the three equations. As in Lemma 2 in Mammen et al. (1999) we conclude from these equations that

$$\|\hat{T}\|_n < \gamma$$

for some $\gamma < 1$ with probability tending to one. Here, we define \hat{T} , $\|\dots\|_n$, $\mathcal{X}_{n,j}$, $\hat{\Psi}_j$, $\tilde{\mathcal{L}}_j$ and $\tilde{\mathcal{L}}$ as T , $\|\dots\|$, \mathcal{X}_j , Ψ_j , \mathcal{L}_j and \mathcal{L} but with O_j, π_{jk} replaced by $\tilde{O}_j, \hat{\pi}_{jk}$ ($0 \leq j, k \leq d; j \neq k$). In particular, we put $\tilde{\mathcal{L}}_j = \{\delta_j : \mathcal{X}_j \rightarrow \mathbb{R} : \int_{\mathcal{X}_j} \delta_j^2(x_j) \tilde{O}_j(x_j) \, dx_j < \infty, \int_{\mathcal{X}_j} \delta_j(x_j) \tilde{O}_j(x_j) \, dx_j = 0\}$,

$\tilde{\mathcal{L}} = \tilde{\mathcal{L}}_1 \times \dots \times \tilde{\mathcal{L}}_d$, and $\|T\|_n = \sup\{\|T(\delta_0 + \dots + \delta_d)\|_n : \delta_j \in \tilde{\mathcal{L}}_j \text{ with } \|\delta_0 + \dots + \delta_d\|_n < 1\}$.

Arguing as in the first part of Lemma 3 in Mammen et al. (1999) this gives that $\bar{\delta}_k(x) = \bar{\delta}_k^A(x) + \bar{\delta}_k^B(x) + \bar{\delta}_k^C(x)$, where for $r \in \{A, B, C\}$ the functions $\bar{\delta}_k^r \in \tilde{\mathcal{L}}_k$ are defined by

$$\bar{\delta}_0^r(x_0) + \dots + \bar{\delta}_d^r(x_d) = \sum_{l=0}^s \hat{T}^l \hat{\tau}^r(x) + \hat{R}^{r,[s]}(x)$$

with $\|\hat{R}^{r,[s]}\| \leq C\gamma^s$ with probability tending to one for some constant $C > 0$. Here we put

$$\begin{aligned} \hat{\tau}^r &= \hat{\Psi}_d \cdot \dots \cdot \hat{\Psi}_1 (\hat{\mu}_0^r - \bar{\mu}_0^{*,r,n}) + \dots + \hat{\Psi}_d (\hat{\mu}_{d-1}^r - \bar{\mu}_{d-1}^{*,r,n}) + (\hat{\mu}_d^r - \bar{\mu}_d^{*,r,n}), \\ \hat{R}^{r,[s]}(x) &= \sum_{l=s+1}^{\infty} \hat{T}^l \hat{\tau}^r(x). \end{aligned}$$

Up to this point we followed closely the arguments in the proof of Theorem 1 in Mammen et al. (1999). The arguments of the further parts of the proof of the latter theorem would need that, in our notation,

$$\sup_{x_j \in \mathcal{X}_j} \int_{\mathcal{X}_{k(x_j)}} \frac{\tilde{O}_{j,k}^2(x_j, x_k)}{\tilde{O}_j^2(x_j) O_k(x_k)} dx_k \quad (\text{B.3})$$

is bounded by a constant, with probability tending to one. This would imply that with probability tending to one for some constant $C > 0$ for all functions $g : \mathcal{X}_{k(x_j)} \rightarrow \mathbb{R}$

$$\sup_{x_j \in \mathcal{X}_j} \left| \int_{\mathcal{X}_{k(x_j)}} \frac{\tilde{O}_{j,k}(x_j, x_k)}{\tilde{O}_j(x_j)} g(x_k) dx_k \right| \leq C \|g\|, \quad (\text{B.4})$$

as can be seen by application of the Cauchy-Schwarz inequality. The proof of Theorem 1 in Mammen et al. (1999) shows that this can be used to show that $\sup_{x \in \mathcal{X}, 0 \leq j \leq d} |R_j^{r,[s]}(x)| \leq C\gamma^s$ with probability tending to one for some constant $C > 0$. Unfortunately in our setting (B.3) does not hold and thus we cannot follow that (B.4) holds in our setting. Indeed, one can

check that in general (B.4) does not hold under our assumptions. Consider e.g. the set-up discussed after the statement of assumption [A7]. Thus we do not have that T and \hat{T} map a function with bounded L_2 -norm into a function with bounded L_∞ -norm. This also does not hold if we replace the L_∞ -norm by our weighted norm $\|\cdot\|_{O,\infty}$. We now argue that after twice application of T or \hat{T} a function with bounded $\|\cdot\|$ -norm is transformed into a function with bounded $\|\cdot\|_{O,\infty}$ -norm. This follows from the following two estimates for functions $g : \mathcal{X}_k \rightarrow \mathbb{R}$ with some constant $C > 0$

$$\int_{\mathcal{X}_j} \left(\int_{\mathcal{X}_k(x_j)} \frac{O_{j,k}(x_j, x_k)}{O_j(x_j)} g(x_k) dx_k \right)^2 O_j^{1-\delta}(x_j) dx_j \leq C \int_{\mathcal{X}_k} O_k(x_k) g^2(x_k) dx_k, \quad (\text{B.5})$$

$$\sup_{x_j \in \mathcal{X}_j} O_j^{1/2}(x_j) \left| \int_{\mathcal{X}_k(x_j)} \frac{O_{j,k}(x_j, x_k)}{O_j(x_j)} g(x_k) dx_k \right| \leq C \left(\int_{\mathcal{X}_k} O_k^{1-\delta}(x_k) g^2(x_k) dx_k \right)^{1/2}. \quad (\text{B.6})$$

Furthermore, it holds with probability tending to one, that

$$\int_{\mathcal{X}_j} \left(\int_{\mathcal{X}_k(x_j)} \frac{\tilde{O}_{j,k}(x_j, x_k)}{\tilde{O}_j(x_j)} g(x_k) dx_k \right)^2 O_j^{1-\delta}(x_j) dx_j \leq C \int_{\mathcal{X}_k} O_k(x_k) g^2(x_k) dx_k, \quad (\text{B.7})$$

$$\sup_{x_j \in \mathcal{X}_j} O_j^{1/2}(x_j) \left| \int_{\mathcal{X}_k(x_j)} \frac{\tilde{O}_{j,k}(x_j, x_k)}{\tilde{O}_j(x_j)} g(x_k) dx_k \right| \leq C \left(\int_{\mathcal{X}_k} O_k^{1-\delta}(x_k) g^2(x_k) dx_k \right)^{1/2}. \quad (\text{B.8})$$

Below we will also use that a function with bounded $\|\cdot\|_{O,\infty}$ -norm is mapped by T and \hat{T} into a function with bounded $\|\cdot\|_{O,\infty}$ -norm. This follows from

$$\sup_{x_j \in \mathcal{X}_j} O_j^{1/2}(x_j) \left| \int_{\mathcal{X}_k(x_j)} \frac{O_{j,k}(x_j, x_k)}{O_j(x_j)} g(x_k) dx_k \right| \leq C^* \sup_{x_k \in \mathcal{X}_k} O_k^{1/2}(x_k) |g(x_k)|, \quad (\text{B.9})$$

$$\sup_{x_j \in \mathcal{X}_j} O_j^{1/2}(x_j) \left| \int_{\mathcal{X}_k(x_j)} \frac{\tilde{O}_{j,k}(x_j, x_k)}{\tilde{O}_j(x_j)} g(x_k) dx_k \right| \leq C^* \sup_{x_k \in \mathcal{X}_k} O_k^{1/2}(x_k) |g(x_k)| \quad (\text{B.10})$$

with probability to one. We now show (B.5)–(B.10). The bound (B.9) follows directly from the last inequality in Condition [A7]. For the proof of (B.5) note that the left hand side of

(B.5) can be bounded by a constant times

$$\int_{\mathcal{X}_{x_j, x_k}} \frac{1}{O_j^{1+\delta}(x_j)O_k(x_k)} dx_j dx_k \int_{\mathcal{X}_k} O_k(x_k)g^2(x_k)dx_k.$$

Thus, (B.5) follows by application of the first inequality in Condition [A7]. For the proof of (B.6) note that the left hand side of (B.6) can be bounded by a constant times

$$\left(\sup_{x_k \in \mathcal{X}_k} \int_{\mathcal{X}_{j(x_k)}} \frac{1}{O_j^{1-\delta}(x_j)O_k(x_k)} dx_j \int_{\mathcal{X}_k} O_k^{1-\delta}(x_k)g^2(x_k)dx_k \right)^{1/2}.$$

Here, (B.6) follows by application of the second inequality in Condition A7. For the proof of (B.7), (B.8) and (B.10) one uses (B.2) to show that the left hand sides of the equations in Condition [A7] are of order $O_P(1)$ if one replaces O_j and O_k by \tilde{O}_j and \tilde{O}_k , respectively. Thus, one can show (B.7), (B.8) and (B.10) by using the same arguments as in the proofs of (B.5), (B.6) and (B.9).

We now want to show that

$$\|\bar{\delta}_0^r(x_0) + \dots + \bar{\delta}_d^r(x_d) - \sum_{l=0}^{\infty} T^l \tau^r(x)\|_{O, \infty} = o_P(n^{-2/5}), \quad (\text{B.11})$$

where

$$\tau^r = \Psi_d \cdot \dots \cdot \Psi_1(\hat{\mu}_0^r - \bar{\mu}_0^{*,r}) + \dots + \Psi_d(\hat{\mu}_{d-1}^r - \bar{\mu}_{d-1}^{*,r}) + (\hat{\mu}_d^r - \bar{\mu}_d^{*,r})$$

and where for $\delta = (\delta^*, \delta_0, \dots, \delta_d)^\top \in \mathbb{R} \times \mathcal{L}$ we define $\|\delta^* + \delta_0 + \dots + \delta_d\|_{O, \infty}$ as $\|(\delta_0, \dots, \delta_d)^\top\|_{O, \infty} \vee |\delta^*|$.

Using (B.5)–(B.10), $\|T\| < 1$ and the fact that $\|\hat{T}\|_n < \gamma$ for some $\gamma < 1$ with probability

tending to one, one gets that for (B.11) it suffices to show that for all choices of $c > 0$

$$\left\| \sum_{l=0}^{c \log n} \widehat{T}^l \widehat{\tau}^r(x) - T^l \tau^r(x) \right\|_{O, \infty} = o_P(n^{-2/5}). \quad (\text{B.12})$$

For the proof of this claim it suffices to show that the norm of each summand is of order $o_P(n^{-2/5}(\log n)^{-1})$. This can be shown by using condition B1, (B.5)–(B.10), and

$$\int_{\mathcal{X}_j} \left(\int_{\mathcal{X}_{k(x_j)}} \left[\frac{\widetilde{O}_{j,k}(x_j, x_k)}{\widetilde{O}_j(x_j)} - \frac{\widetilde{O}_{j,k}(x_j, x_k)}{\widetilde{O}_j(x_j)} \right] g(x_k) dx_k \right)^2 O_j^{1-\delta}(x_j) dx_j \quad (\text{B.13})$$

$$= o_P((\log n)^{-1}) \int_{\mathcal{X}_k} O_k(x_k) g^2(x_k) dx_k,$$

$$\sup_{x_j \in \mathcal{X}_j} O_j^{1/2}(x_j) \left| \int_{\mathcal{X}_{k(x_j)}} \left[\frac{\widetilde{O}_{j,k}(x_j, x_k)}{\widetilde{O}_j(x_j)} - \frac{\widetilde{O}_{j,k}(x_j, x_k)}{\widetilde{O}_j(x_j)} \right] g(x_k) dx_k \right| \quad (\text{B.14})$$

$$= o_P((\log n)^{-1}) \left(\int_{\mathcal{X}_k} O_k^{1-\delta}(x_k) g^2(x_k) dx_k \right)^{1/2},$$

$$\sup_{x_j \in \mathcal{X}_j} O_j^{1/2}(x_j) \left| \int_{\mathcal{X}_{k(x_j)}} \left[\frac{\widetilde{O}_{j,k}(x_j, x_k)}{\widetilde{O}_j(x_j)} - \frac{\widetilde{O}_{j,k}(x_j, x_k)}{\widetilde{O}_j(x_j)} \right] g(x_k) dx_k \right| \quad (\text{B.15})$$

$$= o_P((\log n)^{-1}) \sup_{x_k \in \mathcal{X}_k} O_k^{1/2}(x_k) |g(x_k)|.$$

Claims (B.13)–(B.15) can be shown similarly as (B.5)–(B.10) by using additionally condition [B1].

For $r = B$ we note that $\bar{\mu}_k^{*,r,n} - \bar{\mu}_k^{*,r} = o_P(n^{-2/5})$ because of [B1] and [B4], see also (B.2) and that the sum of the elements of $(I - \pi)^{-1}(\widehat{\mu}^B - \bar{\mu}^{B,*})$ is equal to $\sum_{l=0}^{\infty} T^l \tau^B(x)$. For $r = C$ one checks easily that $\left\| \sum_{l=0}^{\infty} T^l \tau^C \right\|_{O, \infty} = o_P(n^{-2/5})$. For the statement of the proposition it remains to show that $\left\| \sum_{l=1}^{\infty} T^l \tau^A \right\|_{O, \infty} = o_P(n^{-2/5})$ and that $\left\| \tau^r - (\widehat{\mu}_0^r - \bar{\mu}_0^{*,r} + \dots + \widehat{\mu}_d^r - \bar{\mu}_d^{*,r}) \right\|_{O, \infty} = o_P(n^{-2/5})$. For the proof of these two claims one applies condition B5.

B.2 Proof of Proposition 2

The statement of Proposition 2 follows immediately from [B3] and Proposition 1.

B.3 Proof of Theorem 3

The main tool to prove this theorem is the Newton-Kantorovich theorem, see for example Deimling (1985). Since this theorem is central in our considerations we will state it here.

Theorem 4 (Newton-Kantorovich theorem). *Consider Banach spaces \mathcal{X}, \mathcal{Y} and a map $F : B_r(x_0) = \{x : \|x - x_0\| \leq r\} \subset \mathcal{X} \mapsto \mathcal{Y}$ for $x_0 \in \mathcal{X}$ and $r > 0$. We assume that the Fréchet derivative F' exists for $x \in B_r(x_0)$, that it is invertible and that the following conditions are satisfied*

1. $\|F'(x_0)^{-1}F(x_0)\| \leq \gamma$,
2. $\|F'(x_0)^{-1}\| \leq \beta$,
3. $\|F'(x) - F'(x^*)\| \leq l\|x - x^*\|$ for all $x, x^* \in B_r(x_0)$,
4. $2\gamma\beta l < 1$ and $2\gamma < r$.

Then the equation

$$F(x) = 0$$

has a unique solution x^* in $\overline{B}_{2\gamma}(x_0)$ and furthermore, x^* can be approximated by Newtons iterative method

$$x_{k+1} = x_k - F'(x_k)^{-1}F(x_k),$$

and it holds that

$$\|x_k - x^*\| \leq \frac{\gamma}{2^{k-1}}q^{2^k-1}, \quad \text{with } q = 2\gamma\beta l < 1.$$

We now come to the proof of Theorem 3.

Proof of Theorem 3. Equation (A.1) can be rewritten as

$$\widehat{\mathcal{F}}(\widehat{\delta}^*, \widehat{\delta}_0, \dots, \widehat{\delta}_d) = 0,$$

where

$$\widehat{\mathcal{F}}(f^*, f_0, \dots, f_d)(x) = \left(\widehat{\mathcal{F}}_k(f^*, f_0, \dots, f_d)(x) \right)_{k=*,0,\dots,d}.$$

with

$$\begin{aligned} \widehat{\mathcal{F}}_*(f^*, f_0, \dots, f_d)(x) &= \int_{\mathcal{X}} \left[(1 + f^*) \prod_{j=0}^d \{1 + f_j(x_j)\} - 1 \right] \\ &\quad \times \prod_{j=0}^d \alpha_j(x_j) \widehat{E}(x) dx - \int_{\mathcal{X}_k} \widehat{\Delta}_k(x_k) dx_k, \\ \widehat{\mathcal{F}}_k(f^*, f_0, \dots, f_d)(x) &= \int_{\mathcal{X}_{x_k}} \left[(1 + f^*) \prod_{j=0}^d \{1 + f_j(x_j)\} - 1 \right] \\ &\quad \times \prod_{j=0}^d \alpha_j(x_j) \widehat{E}(x) dx_{-k} - \widehat{\Delta}_k(x_k) - \widehat{\mathcal{F}}_*(f^*, f_0, \dots, f_d)(x) \end{aligned}$$

for $k = 0, \dots, d$. Note that $\int_{\mathcal{X}_k} \widehat{\Delta}_k(x_k) dx_k$ does not depend on k .

We define an additional operator \mathcal{F} by the following equations

$$\mathcal{F}(f^*, f_0, \dots, f_d)(x) = (\mathcal{F}_k(f^*, f_0, \dots, f_d)(x))_{k=*,0,\dots,d}$$

with

$$\begin{aligned}
\mathcal{F}_*(f^*, f_0, \dots, f_d)(x) &= \int_{\mathcal{X}} \left[\{1 + f^*\} \prod_{j=0}^d \{1 + f_j(x_j)\} - 1 \right] \\
&\quad \times \prod_{j=0}^d \alpha_j(x_j) E(x) dx, \\
\mathcal{F}_k(f^*, f_0, \dots, f_d)(x) &= \int_{\mathcal{X}_{x_k}} \left[\{1 + f^*\} \prod_{j=0}^d \{1 + f_j(x_j)\} - 1 \right] \\
&\quad \times \prod_{j=0}^d \alpha_j(x_j) E(x) dx_{-k} - \mathcal{F}_*(f^*, f_0, \dots, f_d)(x)
\end{aligned}$$

for $k = 0, \dots, d$.

Note that $\mathcal{F}(0) = 0$. The Fréchet derivatives of $\widehat{\mathcal{F}}$ and \mathcal{F} in 0 are

$$\begin{aligned}
\widehat{\mathcal{F}}'_*(0)(f) &= \int_{\mathcal{X}} \left(f^* + \sum_{j=0}^d f_j(x_j) \right) \alpha(x) \widehat{E}(x) dx, \\
\mathcal{F}'_*(0)(f) &= \int_{\mathcal{X}} \left(f^* + \sum_{j=0}^d f_j(x_j) \right) \alpha(x) E(x) dx, \\
\widehat{\mathcal{F}}'_k(0)(f) &= \int_{\mathcal{X}_{x_k}} \left(f^* + \sum_{j=0}^d f_j(x_j) \right) \alpha(x) \widehat{E}(x) dx_{-k} \\
&\quad - \widehat{\mathcal{F}}'_*(0)(f), \\
\mathcal{F}'_k(0)(f) &= \int_{\mathcal{X}_{x_k}} \left(f^* + \sum_{j=0}^d f_j(x_j) \right) \alpha(x) E(x) dx_{-k} \\
&\quad - \mathcal{F}'_*(0)(f)
\end{aligned}$$

for $k = 0, \dots, d$.

The main idea of our proof is to apply the Newton-Kantorovich theorem, Theorem 4, with the mapping $F = \widehat{\mathcal{F}}$ and norm $\|(f_0, \dots, f_d)\|_{0, \infty} \vee |f^*|$ which in abuse of notation we also denote by $\|(f^*, f_0, \dots, f_d)\|_{0, \infty}$. As starting point x_0 we choose $x_0 = (\bar{\delta}^*, \bar{\delta})$. In our application

of Theorem 4, the spaces \mathcal{X} and \mathcal{Y} are equal to $\mathbb{R} \times \{(f_0, \dots, f_d)^\top : \|(f_0, \dots, f_d)^\top\|_{O, \infty} < \infty, \int f_j(x_j) \tilde{O}_j(x_j) dx_j = 0 \text{ for } j = 0, \dots, d\}$. We consider \mathcal{F} and $\widehat{\mathcal{F}}$ as operators from \mathcal{X} to \mathcal{X} . Note that $\mathcal{F}\mathcal{X} \subset \mathcal{X}$ because of [B6] and the last assumption of [A7]. Note that we get from [B6] and the last assumption of [A7] that

$$\int_{x \in \mathcal{X}} \frac{1}{\prod_{k=0}^d O_k(x_k)^{1/2}} O(x) dx = O(1).$$

Similarly, one uses [B6] and the last assumption of [A7] to show that $\widehat{\mathcal{F}}\mathcal{X} \subset \mathcal{X}$, with probability tending to one.

We will show that

$$\left\| \widehat{\mathcal{F}} \left((\bar{\delta}^*, \bar{\delta}) \right) \right\|_{O, \infty} = o_p(n^{-2/5}), \quad (\text{B.16})$$

and that $\widehat{\mathcal{F}}'$ is locally Lipschitz around 0, i.e., that there exist constants r^*, C such that with probability tending to one

$$\left\| \widehat{\mathcal{F}}'(g)(f) - \widehat{\mathcal{F}}'(g^*)(f) \right\|_{O, \infty} \leq C \|g - g^*\|_{O, \infty} \|f\|_{O, \infty} \quad \text{for all } g, g^* \in B_{r^*}(0). \quad (\text{B.17})$$

Furthermore, we will show, that

$$\mathcal{F}'(0) \text{ is invertible, with } \|\mathcal{F}'(0)^{-1}\|_{O, \infty} < C^*, \quad \text{for some } C^* > 0. \quad (\text{B.18})$$

We now argue that by application of the Newton-Kantorovich theorem (B.16)-(B.18) imply that

$$\left\| (\bar{\delta}^*, \bar{\delta}) - (\widehat{\delta}^*, \widehat{\delta}) \right\|_{O, \infty} = o_p(n^{-2/5}). \quad (\text{B.19})$$

This implies the statement of the theorem.

We now show that (B.16)-(B.18) imply (B.19). Since $\left\|(\bar{\delta}^*, \bar{\delta})\right\|_{O,\infty} = o_P(1)$, the inequality (B.17) also holds with a constant r for all $g, g^* \in B_r\left((\bar{\delta}^*, \bar{\delta})\right)$ with probability tending to one. This gives condition (c) of the Newton-Kantorovich theorem.

Furthermore, by application of (B.2) we get that $\left\|\widehat{\mathcal{F}}'(0) - \mathcal{F}'(0)\right\|_{O,\infty} = o_P(1)$. This together with $\left\|(\bar{\delta}^*, \bar{\delta})\right\|_{O,\infty} = o_P(1)$ and (B.17) gives

$$\left\|\widehat{\mathcal{F}}'\left((\bar{\delta}^*, \bar{\delta})\right) - \mathcal{F}'(0)\right\|_{O,\infty} = o_p(1).$$

Therefore with probability tending to one, condition (B.18) also holds if $\mathcal{F}'(0)$ is replaced by $\widehat{\mathcal{F}}'\left((\bar{\delta}^*, \bar{\delta})\right)$. Thus, we get from (B.16)-(B.18) that conditions (a)-(d) of the Newton-Kantorovich theorem are fulfilled with probability tending to one, with $\gamma = o_P(n^{-2/5})$. This shows (B.19).

It remains to show (B.16), (B.17) and (B.18). For the proof of (B.16) note that $\left\|(\bar{\delta}^*, \bar{\delta})\right\|_{O,\infty} = o_p(n^{-1/5})$ and that $\widehat{\mathcal{F}}'$ is Lipschitz. A first order Taylor expansion yields

$$\widehat{\mathcal{F}}(\bar{\delta}) = \widehat{\mathcal{F}}(0) + \widehat{\mathcal{F}}'(0)\left((\bar{\delta}^*, \bar{\delta})\right) + o_p(n^{-2/5}).$$

Equation (B.16) follows from $\widehat{\mathcal{F}}(0) + \widehat{\mathcal{F}}'(0)\left((\bar{\delta}^*, \bar{\delta})\right) = \widehat{\mathcal{F}}(0) - \widehat{\mathcal{F}}(0) = 0$.

Claim (B.17) follows directly from assumption [B6].

For the proof of (B.18) we have to show that $\mathcal{F}'(0)$ is invertible. For the proof of this claim we start by showing that it is bijective. For the proof of injectivity, assume that $\mathcal{F}'(0)(f) = 0$ for some $f = (f^*, f_0, \dots, f_d)^\top \in \mathcal{X}$. We will show that this implies that $f = 0$.

It holds that

$$\int_{\mathcal{X}} \left(f^* + \sum_{j=0}^d f_j(x_j) \right) \alpha(x) E(x) dx = 0,$$

$$\int_{\mathcal{X}_{x_k}} \left(f^* + \sum_{j=0}^d f_j(x_j) \right) \alpha(x) E(x) dx_{-k} = 0, \quad \text{for all } k = 0, \dots, d.$$

With $\bar{f}_j(x_j) = f_j(x_j) - \int f_j(u_j) v(u) du$ and $\bar{f}^* = f^* + \sum_{j=0}^d \int f_j(u_j) v(u) du$ for $v(u) = \alpha(u) E(u) / \int \alpha(s) E(s) ds$ this implies that

$$\bar{f}^* \int_{\mathcal{X}} \alpha(x) E(x) dx = 0$$

and thus it holds that $\bar{f}^* = 0$. Furthermore, we get that for $k = 0, \dots, d$

$$0 = \int_{\mathcal{X}_k} \bar{f}_k(x_k) \int_{\mathcal{X}_{x_k}} \left(\sum_{j=0}^d \bar{f}_j(x_j) \right) \alpha(x) E(x) dx_{-k} dx_k = \int_{\mathcal{X}} \bar{f}_k(x_k) \left(\sum_{j=0}^d \bar{f}_j(x_j) \right) \alpha(x) E(x) dx.$$

By summing these terms up over k , we get that

$$\int_{\mathcal{X}} \left\{ \sum_{j=0}^d \bar{f}_j(x_j) \right\}^2 \alpha(x) E(x) dx = 0,$$

which implies that

$$\sum_{j=0}^d \bar{f}_j(x_j) = 0, \quad \text{a.e. on } \mathcal{X}.$$

By application of (B.1) this implies that \bar{f}_j and f_j are constant functions. Because of $\int f_j(u_j) \alpha(u) \widehat{E}(u) du = 0$ this implies $f = 0$.

Now we check that $\mathcal{F}'(0)$ is surjective. Consider $g = (g^*, g_0, \dots, g_d)^\top \in \mathcal{X}$ such that

$$\langle \mathcal{F}'(0)(f), g \rangle = \mathcal{F}'_*(0)(f)g^* + \sum_{k=0}^d \int_{\mathcal{X}_k} \mathcal{F}'_k(0)(f)(x_k)g_k(x_k)dx_k = 0 \quad (\text{B.20})$$

for all $f = (f^*, f_0, \dots, f_d)^\top \in \mathcal{X}$. We will show that then $g = 0$. This implies that $g = 0$ is the only element in \mathcal{Y} that is perpendicular to the range space of $\mathcal{F}'(0)$. Since $\mathcal{F}'(0)$ is linear, this shows that $\mathcal{F}'(0)$ is surjective.

From (B.20) one gets with the choice $f_k = g_k$ and $f^* = g^*$ that

$$\begin{aligned} 0 &= (g^*)^2 \int_{\mathcal{X}} \alpha(x)E(x)dx + \sum_{k=0}^d \int_{\mathcal{X}_k} g_k(x_k) \int_{\mathcal{X}_{x_k}} \left(\sum_{j=0}^d g_j(x_j) \right) \alpha(x)E(x)dx_{-k}dx_k \\ &= (g^*)^2 \int_{\mathcal{X}} \alpha(x)E(x)dx + \int_{\mathcal{X}} \left(\sum_{j=0}^d g_j(x_j) \right)^2 \alpha(x)E(x)dx. \end{aligned}$$

With exactly the same arguments as for the injectivity we conclude that $g = 0$ and that $g^* = 0$. Thus, we have shown that $\mathcal{F}'(0)$ is invertible.

It remains to show that $\mathcal{F}'(0)^{-1}$ is bounded. By the bounded inverse theorem for this claim it suffices to show that $\mathcal{F}'(0)$ is bounded. Boundedness of $\mathcal{F}'(0)$ can be shown by application of (B.10). This concludes the proof of Theorem 3. \square

C Simulation results

C.0.1 Simulation study of Honda (2005) and Lin et al. (2016)

In this section we present the simulation results of our proposed smooth backfitting estimator in the setting of Honda (2005) and Lin et al. (2016). We refer to Lin et al. (2016) for notation and simulation setting. We only present the results for Model 1 and Model 2 (not Model

3) of Lin et al. (2016), because in Model 3, Lin et al. (2016) estimate η 's by over-smoothing (bandwidth is double the size of the support) their local linear estimator. Hence, if over-smoothing is done because of the knowledge of an underlying linear function, then using the (linear) Cox proportional hazard model is actually more appropriate.

In each model, the last two rows of Table 3 show the results of a simulation (with 1000 repetitions) run by us; the first five rows are copied from Table 3 in Lin et al. (2016). We conclude that our proposed estimator, in the setting considered, shares top performance together with Lin et al. (2016), with all other estimators showing inferior performance.

Method	$z = 0.5$			$z = -0.5$		
	Bias	SD	RMSE	Bias	SD	RMSE
Model 1						
Huang (1999)	0.0409	0.2006	0.2048	0.0467	0.2181	0.2230
Fan et al. (1997)	-0.1006	0.2502	0.2697	-0.1267	0.1879	0.2265
Linton et al. (2003)	-0.0350	0.2949	0.2970	0.0400	0.2702	0.2731
Honda (2005)	0.1130	0.2588	0.2824	-0.1090	0.2569	0.2791
Lin et al. (2016) (copied)	-0.0381	0.1380	0.1432	0.0881	0.1558	0.1790
Lin et al. (2016) (re-run)	0.0389	0.0990	0.1061	0.0394	0.1042	0.1111
SBF	0.0803	0.1018	0.1293	0.08148	0.10253	0.1306
Model 2						
Huang (1999)	0.0457	0.2066	0.2116	-0.0014	0.2116	0.2116
Fan et al. (1997)	0.0168	0.2995	0.2999	0.1662	0.2506	0.3007
Linton et al. (2003)	-0.0560	0.3209	0.3257	0.0780	0.3049	0.3147
Honda (2005)	0.1040	0.2302	0.2526	-0.1060	0.2408	0.2631
Lin et al. (2016) (copied)	0.0621	0.0606	0.0868	-0.0372	0.0901	0.0975
Lin et al. (2016) (re-run)	-0.0660	0.1488	0.1630	-0.0697	0.1450	0.1606
SBF	-0.0038	0.1463	0.1463	-0.0098	0.1376	0.1375

Table 3: Summaries of the simulation results in the setting of Honda (2005) and Lin et al. (2016). In each model, the last two rows show the results of a simulation (with 1000 repetitions) run by us; the first five rows are copied from Table 1 in Lin et al. (2016).

C.1 Additional simulation results in the setting of the main manuscript

In this section we present additional simulation results for the simulation study conducted in the main manuscript. We refer to the main manuscript for notation and simulation setting.

C.2 Dimension $d = 2$

Number of breakdowns in Lin et al. (2016) for $d = 2$ (out of 200 simulations)						
	Model 1			Model 2		
	$\rho = 0$	$\rho = 0.5$	$\rho = 0.8$	$\rho = 0$	$\rho = 0.5$	$\rho = 0.8$
n=200	0	1	2	0	0	0
n=500	0	0	0	0	0	0

Table 4: Number of breakdowns in the algorithm of Lin et al. (2016) out of 200 simulations for dimension $d = 2$.

ISE values for Model 1 (d=2)								
			Lin et al. (2016)			SBF		
sample size	correlation	component	mean	median	sd	mean	median	sd
n=200	$\rho = 0$	$k = 1$	0.074	0.059	0.059	0.052	0.039	0.048
		$k = 2$	0.087	0.068	0.063	0.058	0.045	0.048
	$\rho = 0.5$	$k = 1$	0.077	0.060	0.055	0.061	0.047	0.048
		$k = 2$	0.087	0.068	0.069	0.058	0.044	0.044
	$\rho = 0.8$	$k = 1$	0.128	0.094	0.112	0.089	0.075	0.062
		$k = 2$	0.136	0.096	0.120	0.088	0.071	0.057
n=500	$\rho = 0$	$k = 1$	0.026	0.022	0.019	0.019	0.015	0.016
		$k = 2$	0.033	0.027	0.026	0.026	0.021	0.020
	$\rho = 0.5$	$k = 1$	0.027	0.021	0.020	0.023	0.018	0.017
		$k = 2$	0.032	0.026	0.023	0.029	0.025	0.021
	$\rho = 0.8$	$k = 1$	0.041	0.030	0.040	0.048	0.043	0.028
		$k = 2$	0.051	0.037	0.048	0.055	0.051	0.030

Table 5: Summaries for integrated squared errors. Simulations where the algorithm of Lin et al. (2016) broke down are taken out.

ISE values for Model 2 (d=2)								
sample size	correlation	component	Lin et al. (2016)			SBF		
			mean	median	sd	mean	median	sd
n=200	$\rho = 0$	$k = 1$	0.120	0.109	0.068	0.132	0.105	0.085
		$k = 2$	0.080	0.065	0.059	0.066	0.052	0.058
	$\rho = 0.5$	$k = 1$	0.151	0.127	0.088	0.159	0.124	0.113
		$k = 2$	0.079	0.064	0.060	0.072	0.063	0.047
	$\rho = 0.8$	$k = 1$	0.303	0.236	0.242	0.172	0.153	0.105
		$k = 2$	0.140	0.089	0.146	0.090	0.080	0.062
n=500	$\rho = 0$	$k = 1$	0.086	0.078	0.041	0.105	0.092	0.053
		$k = 2$	0.031	0.025	0.021	0.027	0.022	0.020
	$\rho = 0.5$	$k = 1$	0.104	0.099	0.047	0.111	0.098	0.055
		$k = 2$	0.030	0.025	0.019	0.036	0.031	0.021
	$\rho = 0.8$	$k = 1$	0.199	0.185	0.092	0.135	0.124	0.062
		$k = 2$	0.046	0.036	0.032	0.061	0.056	0.033

Table 6: Summaries for integrated squared errors. Simulations where the algorithm of Lin et al. (2016) broke down are taken out.

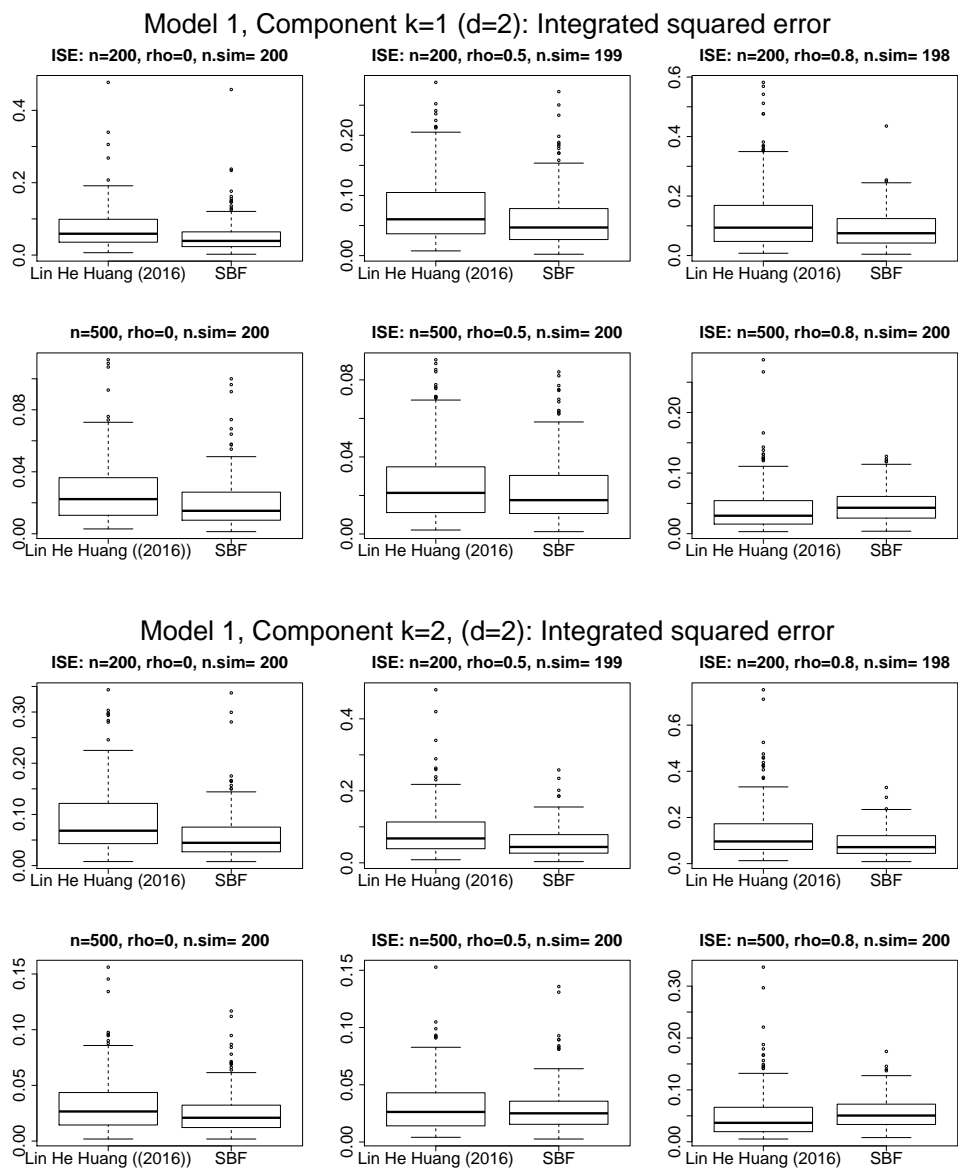


Figure 8: Boxplots of the integrated squared errors. Simulations where the algorithm of Lin et al. (2016) broke down are taken out. The value $n.sim$ is the number of successful simulations, i.e., 200 minus number of break downs.

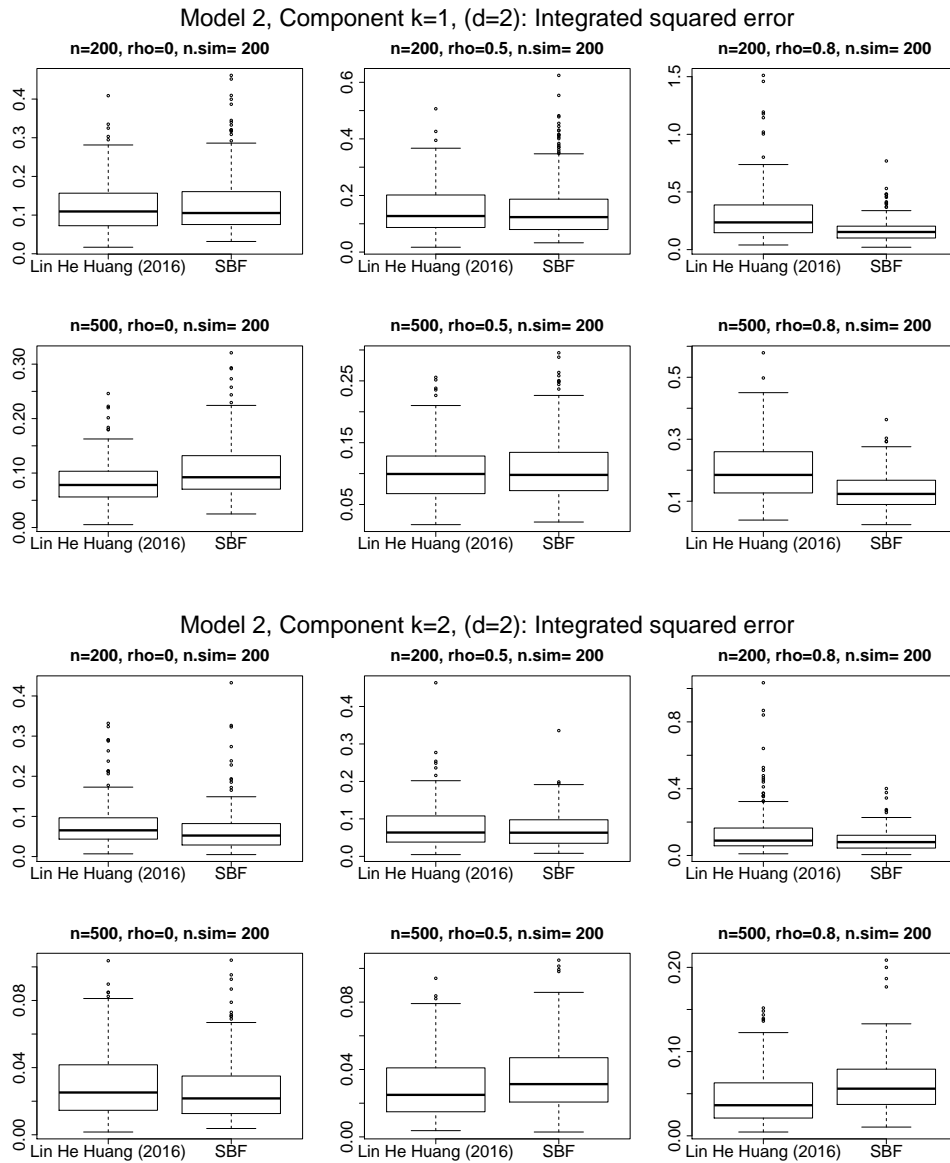


Figure 9: Boxplots of the integrated squared errors. Simulations where the algorithm of Lin et al. (2016) broke down are taken out. The value $n.sim$ is the number of successful simulations, i.e., 200 minus number of break downs.

C.2.1 Dimension $d = 9$

Number of breakdowns in Lin et al. (2016) for $d = 9$ (out of 200 simulations)						
	Model 1			Model 2		
	$\rho = 0$	$\rho = 0.5$	$\rho = 0.8$	$\rho = 0$	$\rho = 0.5$	$\rho = 0.8$
n=200	4	5	48	0	0	9
n=500	0	1	1	0	0	0

Table 7: Number of breakdowns in the algorithm of Lin et al. (2016) out of 200 simulations for dimension $d = 9$.

ISE values for Model 1 (d=9)								
			Lin et al. (2016)			SBF		
sample size	correlation	component	mean	median	sd	mean	median	sd
n=200	$\rho = 0$	$k = odd$	0.119	0.095	0.100	0.056	0.043	0.049
		$k = even$	0.166	0.124	0.154	0.063	0.048	0.057
	$\rho = 0.5$	$k = odd$	0.164	0.121	0.151	0.072	0.057	0.056
		$k = even$	0.228	0.155	0.256	0.078	0.061	0.060
	$\rho = 0.8$	$k = odd$	0.362	0.256	0.534	0.117	0.096	0.090
		$k = even$	0.443	0.282	0.476	0.137	0.113	0.106
n=500	$\rho = 0$	$k = odd$	0.032	0.026	0.024	0.022	0.016	0.019
		$k = even$	0.041	0.032	0.032	0.027	0.022	0.021
	$\rho = 0.5$	$k = odd$	0.041	0.032	0.031	0.032	0.027	0.022
		$k = even$	0.048	0.035	0.040	0.038	0.032	0.026
	$\rho = 0.8$	$k = odd$	0.091	0.063	0.087	0.061	0.052	0.041
		$k = even$	0.107	0.071	0.112	0.077	0.068	0.047

Table 8: Summaries for integrated squared errors. Simulations where the algorithm of Lin et al. (2016) broke down are taken out.

ISE values for Model 2 (d=9)								
sample size	correlation	component	Lin et al. (2016)			SBF		
			mean	median	sd	mean	median	sd
n=200	$\rho = 0$	$k = odd$	0.302	0.284	0.122	0.216	0.194	0.115
		$k = even$	0.134	0.116	0.083	0.104	0.086	0.077
	$\rho = 0.5$	$k = odd$	0.372	0.343	0.167	0.218	0.184	0.143
		$k = even$	0.133	0.107	0.099	0.126	0.106	0.085
	$\rho = 0.8$	$k = odd$	0.821	0.664	0.561	0.252	0.210	0.163
		$k = even$	0.297	0.196	0.331	0.211	0.184	0.124
n=500	$\rho = 0$	$k = odd$	0.286	0.281	0.063	0.166	0.156	0.062
		$k = even$	0.109	0.104	0.042	0.057	0.051	0.033
	$\rho = 0.5$	$k = odd$	0.311	0.310	0.076	0.157	0.144	0.073
		$k = even$	0.080	0.072	0.042	0.072	0.063	0.042
	$\rho = 0.8$	$k = odd$	0.571	0.540	0.205	0.189	0.166	0.096
		$k = even$	0.085	0.064	0.075	0.150	0.141	0.064

Table 9: Summaries for integrated squared errors. Simulations where the algorithm of Lin et al. (2016) broke down are taken out.

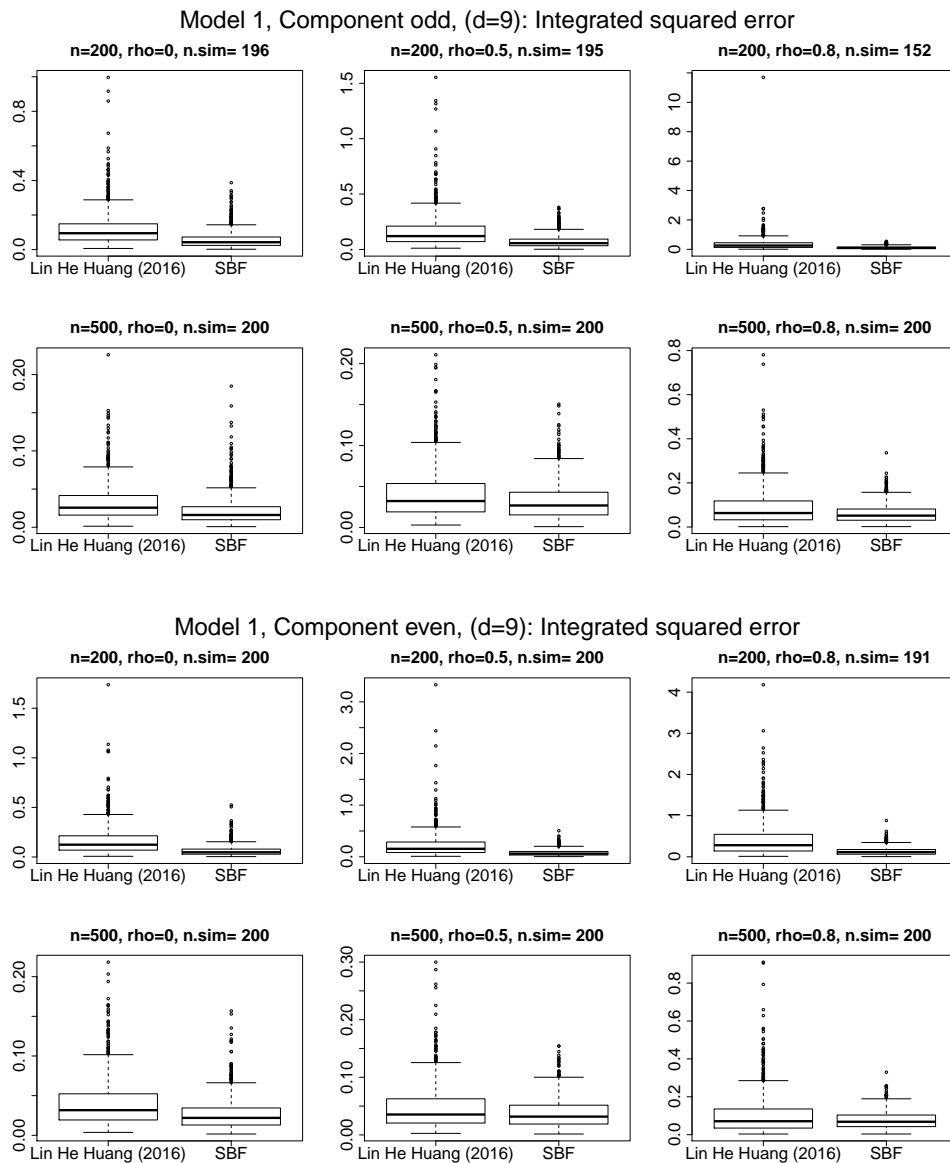


Figure 10: Boxplots of the integrated squared errors in Model 1. Simulations where the algorithm of Lin et al. (2016) broke down are taken out. The value $n.sim$ is the number of successful simulations, i.e., 200 minus number of break downs.

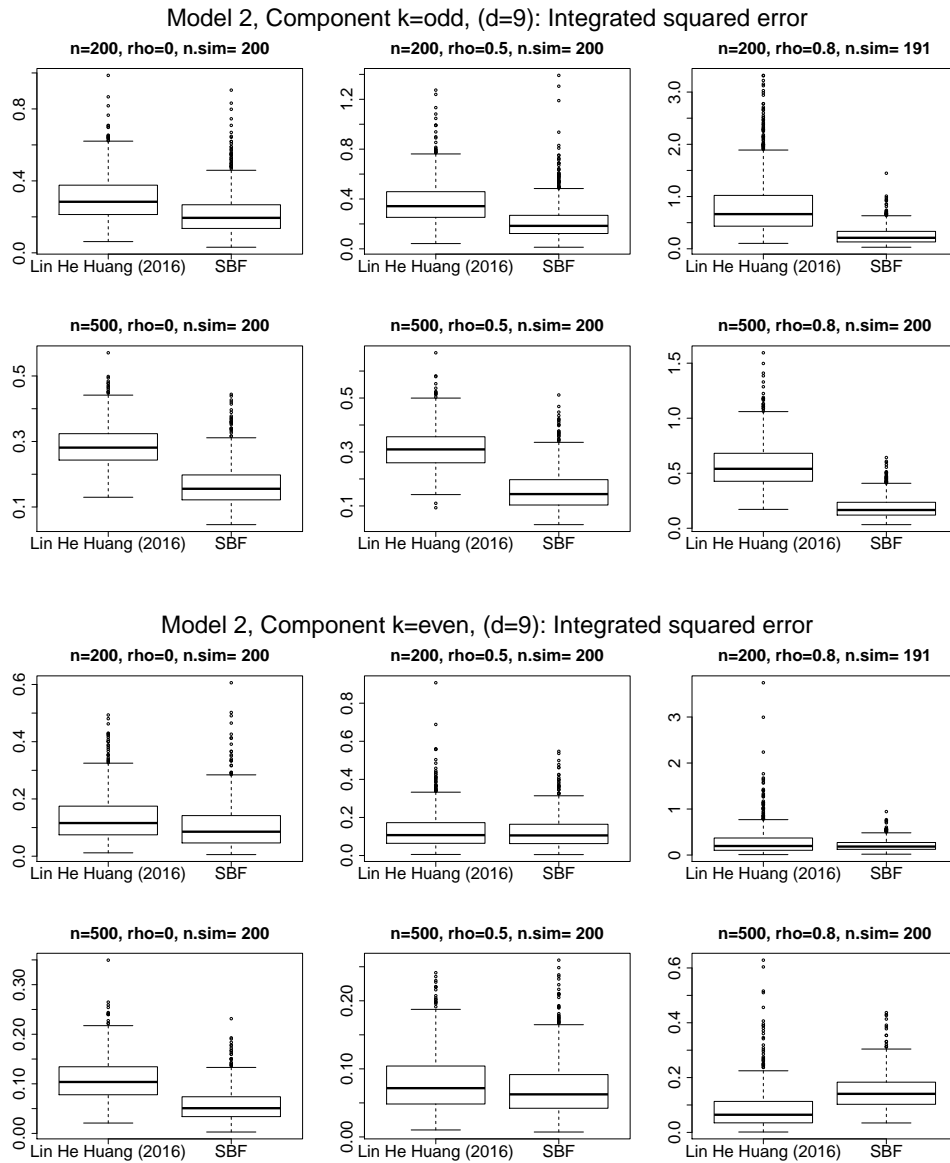


Figure 11: Boxplots of the integrated squared errors in Model 2. Simulations where the algorithm of Lin et al. (2016) broke down are taken out. The value $n.sim$ is the number of successful simulations, i.e., 200 minus number of break downs.

C.2.2 Dimension $d = 30$

Number of breakdowns in Lin et al. (2016) for $d = 30$ (out of 200 simulations)						
	Model 1			Model 2		
	$\rho = 0$	$\rho = 0.5$	$\rho = 0.8$	$\rho = 0$	$\rho = 0.5$	$\rho = 0.8$
n=200	106	176	200	2	67	96
n=500	2	2	47	0	0	7

Table 10: Number of breakdowns in the algorithm of Lin et al. (2016) out of 200 simulations for dimension $d = 30$.

ISE values for Model 1 (d=30)								
			Lin et al. (2016)			SBF		
sample size	correlation	component	mean	median	sd	mean	median	sd
n=200	$\rho = 0$	$k = odd$	0.406	0.295	0.368	0.078	0.061	0.065
		$k = even$	0.741	0.571	0.635	0.098	0.082	0.072
	$\rho = 0.5$	$k = odd$	0.664	0.481	0.625	0.107	0.091	0.079
		$k = even$	1.092	0.759	1.024	0.128	0.099	0.104
	$\rho = 0.8$	$k = odd$	NA	NA	NA	NA	NA	NA
		$k = even$	NA	NA	NA	NA	NA	NA
n=500	$\rho = 0$	$k = odd$	0.073	0.055	0.059	0.030	0.023	0.023
		$k = even$	0.146	0.108	0.127	0.048	0.041	0.031
	$\rho = 0.5$	$k = odd$	0.106	0.079	0.095	0.051	0.043	0.035
		$k = even$	0.185	0.135	0.180	0.065	0.057	0.040
	$\rho = 0.8$	$k = odd$	0.283	0.182	0.285	0.099	0.088	0.059
		$k = even$	0.382	0.234	0.478	0.122	0.111	0.067

Table 11: Summaries for integrated squared errors. Simulations where the algorithm of Lin et al. (2016) broke down are taken out.

ISE values for Model 2 (d=30)								
sample size	correlation	component	Lin et al. (2016)			SBF		
			mean	median	sd	mean	median	sd
n=200	$\rho = 0$	$k = odd$	0.766	0.724	0.329	0.431	0.397	0.200
		$k = even$	0.312	0.264	0.221	0.210	0.176	0.149
	$\rho = 0.5$	$k = odd$	1.153	0.939	0.750	0.341	0.288	0.220
		$k = even$	0.526	0.354	0.554	0.213	0.175	0.150
	$\rho = 0.8$	$k = odd$	3.089	2.634	2.437	0.379	0.380	0.203
		$k = even$	2.176	1.653	1.875	0.340	0.312	0.179
n=500	$\rho = 0$	$k = odd$	0.643	0.637	0.101	0.329	0.316	0.101
		$k = even$	0.258	0.254	0.068	0.136	0.127	0.067
	$\rho = 0.5$	$k = odd$	0.711	0.699	0.143	0.211	0.186	0.116
		$k = even$	0.224	0.214	0.098	0.119	0.103	0.075
	$\rho = 0.8$	$k = odd$	1.250	1.152	0.512	0.270	0.241	0.144
		$k = even$	0.253	0.186	0.241	0.220	0.205	0.098

Table 12: Summaries for integrated squared errors. Simulations where the algorithm of Lin et al. (2016) broke down are taken out.

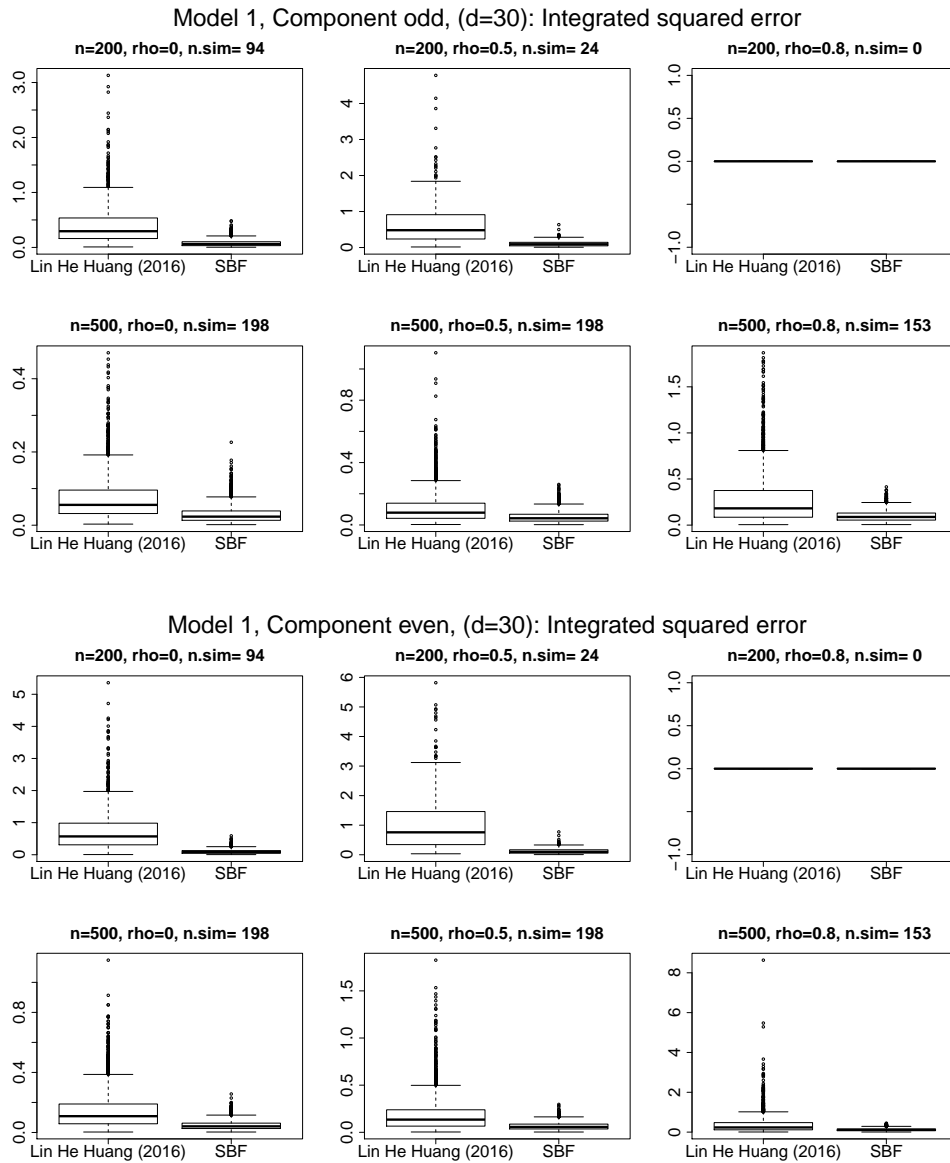


Figure 12: Boxplots of the integrated squared errors in Model 1. Simulations where the algorithm of Lin et al. (2016) broke down are taken out. The value $n.sim$ is the number of successful simulations, i.e., 200 minus number of break downs.

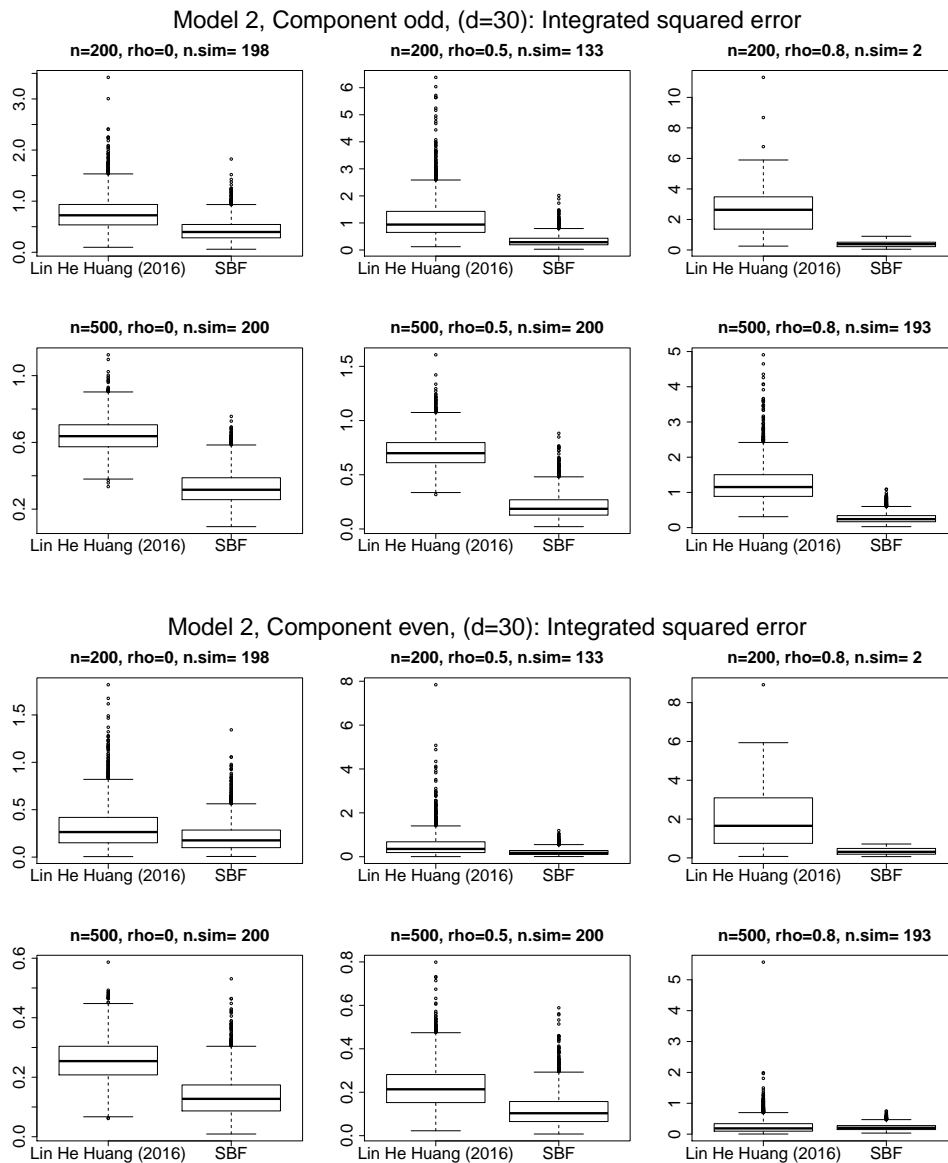


Figure 13: Boxplots of the integrated squared errors in Model 2. Simulations where the algorithm of Lin et al. (2016) broke down are taken out. The value $n.sim$ is the number of successful simulations, i.e., 200 minus number of break downs.

C.2.3 Dimension $d = 99$

Number of breakdowns in Lin et al. (2016) for $d = 99$ (out of 200 simulations)				
	Model 1		Model 2	
	$\rho = 0$	$\rho = 0.5$	$\rho = 0$	$\rho = 0.5$
n=200	200	200	200	200
n=500	180	200	13	194

Table 13: Number of breakdowns in the algorithm of Lin et al. (2016) out of 200 simulations for dimension $d = 99$.

ISE values for Model 1 (d=99)								
			Lin et al. (2016)			SBF		
sample size	correlation	component	mean	median	sd	mean	median	sd
n=500	$\rho = 0$	$k = odd$	0.394	0.290	0.359	0.064	0.052	0.046
		$k = even$	0.744	0.578	0.525	0.136	0.122	0.075

Table 14: Summaries for integrated squared errors. Simulations where the algorithm of Lin et al. (2016) broke down are taken out.

ISE values for Model 2 (d=99)								
			Lin et al. (2016)			SBF		
sample size	correlation	component	mean	median	sd	mean	median	sd
n=500	$\rho = 0$	$k = odd$	1.361	1.289	0.476	0.738	0.710	0.246
		$k = even$	0.570	0.497	0.378	0.350	0.326	0.180
n=500	$\rho = 0.5$	$k = odd$	1.657	1.505	0.785	0.330	0.288	0.194
		$k = even$	0.659	0.485	0.643	0.208	0.179	0.134

Table 15: Summaries for integrated squared errors. Simulations where the algorithm of Lin et al. (2016) broke down are taken out.

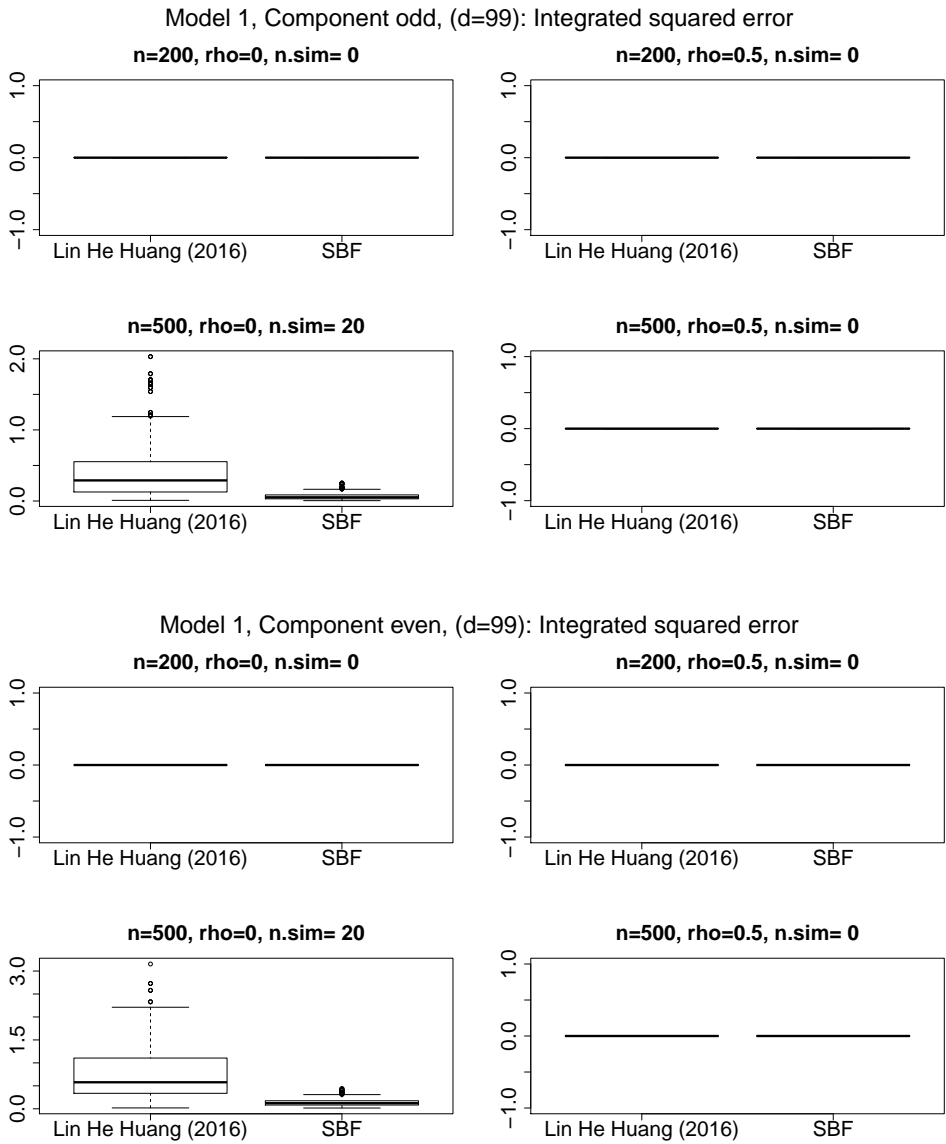


Figure 14: Boxplots of the integrated squared errors in Model 1. Simulations where the algorithm of Lin et al. (2016) broke down are taken out. The value $n.sim$ is the number of successful simulations, i.e., 200 minus number of break downs.

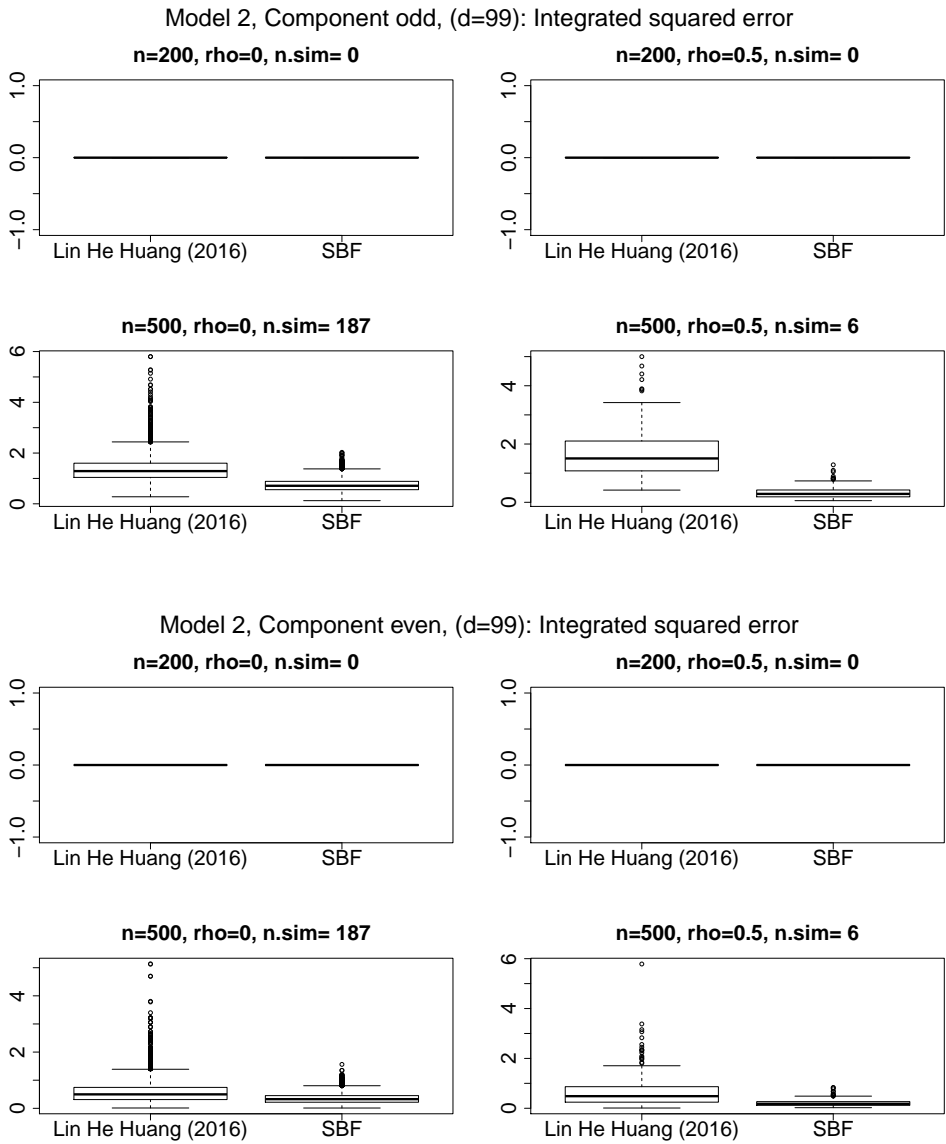


Figure 15: Boxplots of the integrated squared errors in Model 2. Simulations where the algorithm of Lin et al. (2016) broke down are taken out. The value $n.sim$ is the number of successful simulations, i.e., 200 minus number of break downs.

D Bandwidth selection

A crucial problem in practice is finding the right amount of smoothing when using non-parametric approaches. In the application described in this paper we have considered the maybe most straightforward way to estimate the optimal bandwidth – the data-driven cross-validation method.

The data-driven cross-validation method in density estimation goes back to Rudemo (1982) and Bowman (1984). Nowadays, a slightly modified version (see Hall (1983)) is used which aims to minimize the integrated squared error. In our framework, the cross-validation bandwidth has been proposed in Nielsen and Linton (1995). Cross-validation arises from the idea to minimize the integrated squared error

$$n^{-1} \sum_{i=1}^n \int_0^{R_0} [\hat{\alpha}\{X_i(s)\} - \alpha\{X_i(s)\}]^2 Y_i(s) ds.$$

By expanding the square, only two of the three terms depend on the bandwidth and are thus considered. While $\int \hat{\alpha}(X_i(s))^2 ds$ is feasible, we have to estimate $\sum_i \int \hat{\alpha}(X_i(s))\alpha(X_i(s))Y_i(s) ds$. In cross-validation this is done by the unbiased leave-one-out estimator

$$\int \hat{\alpha}^{[i]}\{X_i(s)\} dN_i(s),$$

where $\hat{\alpha}^{[i]}$ is the leave-one-out version, which arises from the definition of structured estimator $\hat{\alpha}$ by setting $N_i = 0$. Finally we define the cross-validated bandwidth, b_{CV} , as

$$b_{CV} = \arg \min_b \sum_{i=1}^n \int \hat{\alpha}(X_i(s))^2 ds - 2 \sum_{i=1}^n \int \hat{\alpha}^{[i]}\{X_i(s)\} dN_i(s). \quad (\text{D.1})$$

Theoretical properties of cross-validation in hazard estimation in the one dimensional case are derived in Mammen et al. (2015). To our knowledge there is no theoretical analysis of

cross-validation in the multivariate hazard case of this paper. An extensive simulation study of the multivariate case can be found in Gámiz et al. (2013).

References

- Andersen, P., O. Borgan, R. Gill, and N. Keiding (1993). *Statistical Models Based on Counting Processes*. New York: Springer.
- Bowman, A. W. (1984). An alternative method of cross-validation for the smoothing of density estimates. *Biometrika* 71, 353–360.
- Breiman, L. (2001). Random forests. *Machine learning* 45, 5–32.
- Deimling, K. (1985). *Nonlinear functional analysis*. Berlin: Springer.
- Fan, J., I. Gijbels, and M. King (1997). Local likelihood and local partial likelihood in hazard regression. *Ann. Stat.* 25, 1661–1690.
- Gámiz, M. L., L. Janys, M. D. Martínez-Miranda, and J. P. Nielsen (2013). Bandwidth selection in marker dependent kernel hazard estimation. *Comput. Stat. Data An.* 68, 155–169.
- Grambsch, P. M., T. M. Therneau, and T. R. Fleming (1995). Diagnostic plots to reveal functional form for covariates in multiplicative intensity models. *Biometrics* 51, 1469–1482.
- Hall, P. (1983). Large sample optimality of least squares cross-validation in density estimation. *Ann. Stat.* 11, 1156–1174.
- Hastie, T. J. and R. J. Tibshirani (1990a). *Generalized Additive Models*. London: Chapman and Hall.
- Hastie, T. J. and R. J. Tibshirani (1990b). Exploring the nature of covariate effects in the proportional hazards model. *Biometrics* 46, 1005–1016.
- Hiabu, M. (2017). On the relationship between classical chain ladder and granular reserving. *Scand. Actuar. J.* 2017, 708–729.

- Hiabu, M., E. Mammen, M. D. Martínez-Miranda, and J. P. Nielsen (2016). In-sample forecasting with local linear survival densities. *Biometrika* 103, 843–859.
- Honda, T. (2005). Estimation in additive cox models by marginal integration. *Annals of the Institute of Statistical Mathematics* 57, 403–423.
- Hsu, L., M. Gorfine, and D. Zucker (2018). On estimation of the hazard function from population-based case–control studies. *Journal of the American Statistical Association* 113, 560–570.
- Huang, J. (1999). Efficient estimation of the partly linear additive cox model. *The Annals of Statistics* 27, 1536–1563.
- Huang, L.-S. and C.-H. Yu (2019). Classical backfitting for smooth-backfitting additive models. *Journal of Computational and Graphical Statistics* 28, 386–400.
- Jones, M. C. (1993). Simple boundary correction for kernel density estimation. *Statistics and computing* 3, 135–146.
- Lee, Y. K., E. Mammen, J. P. Nielsen, and B. U. Park (2015). Asymptotics for in-sample density forecasting. *Ann. Stat.* 43, 620–651.
- Lee, Y. K., E. Mammen, J. P. Nielsen, and B. U. Park (2017). Operational time and in-sample density forecasting. *Ann. Stat.* 45, 1312–1341.
- Lee, Y. K., E. Mammen, J. P. Nielsen, and B. U. Park (2018). In-sample forecasting: A brief review and new algorithms. *ALEA-Latin American Journal of Probability and Mathematical Statistics* 15, 875–895.
- Lin, H., Y. He, and J. Huang (2016). A global partial likelihood estimation in the additive cox proportional hazards model. *J. Statist. Plann. Inference* 169, 71–87.

- Linton, O. B. and J. P. Nielsen (1995). A kernel method of estimating structured nonparametric regression based on marginal integration. *Biometrika* 82, 93–100.
- Linton, O. B., J. P. Nielsen, and S. Van de Geer (2003). Estimating multiplicative and additive hazard functions by kernel methods. *Ann. Stat.* 31, 464–492.
- Mammen, E., O. B. Linton, and J. P. Nielsen (1999). The existence and asymptotic properties of a backfitting projection algorithm under weak conditions. *Ann. Stat.* 27, 1443–1490.
- Mammen, E., J. S. Marron, B. A. Turlach, and M. P. Wand (2001). A general projection framework for constrained smoothing. *Statistical Science* 16, 232–248.
- Mammen, E., M. D. Martínez-Miranda, and J. P. Nielsen (2015). In-sample forecasting applied to reserving and mesothelioma. *Insurance Math. Econom.* 61, 76–86.
- Martínez-Miranda, M. D., J. P. Nielsen, S. Sperlich, and R. Verrall (2013). Continuous chain ladder: Reformulating and generalising a classical insurance problem. *Expert. Syst. Appl.* 40, 5588–5603.
- Nielsen, J. P. (1998). Marker dependent kernel hazard estimation from local linear estimation. *Scand. Actuar. J.* 1998, 113–124.
- Nielsen, J. P. and O. B. Linton (1995). Kernel estimation in a non-parametric marker dependent hazard model. *Ann. Stat.* 23, 1735–1748.
- Nielsen, J. P. and S. Sperlich (2005). Smooth backfitting in practice. *Journal of the Royal Statistical Society: Series B (Statistical Methodology)* 67, 43–61.
- Nielsen, J. P. and C. Tanggaard (2001). Boundary and bias correction in kernel hazard estimation. *Scand. J. Stat.* 28, 675–698.

- OSullivan, F. (1988). Nonparametric estimation of relative risk using splines and cross-validation. *SIAM Journal on Scientific and Statistical Computing* 9, 531–542.
- OSullivan, F. (1993). Nonparametric estimation in the cox model. *The Annals of Statistics* 21, 124–145.
- Rudemo, M. (1982). Empirical choice of histograms and kernel density estimators. *Scand. J. Stat.* 9, 65–78.
- Sleeper, L. A. and D. P. Harrington (1990). Regression splines in the cox model with application to covariate effects in liver disease. *Journal of the American Statistical Association* 85(412), 941–949.
- Stone, C. J. (1982). Optimal global rates of convergence for nonparametric regression. *Ann. Stat.* 10, 1040–1053.
- Therneau, T. M., P. M. Grambsch, and T. R. Fleming (1990). Martingale-based residuals for survival models. *Biometrika* 77, 147–160.
- Wright, M. N. and A. Ziegler (2017). ranger: A fast implementation of random forests for high dimensional data in c++ and r. *Journal of Statistical Software, Articles* 77, 1–17.
- Yu, K., B. U. Park, and E. Mammen (2008). Smooth backfitting in generalized additive models. *Ann. Stat.* 36, 228–260.